Ray theoretical depth migration : methodology and application to deep seismic reflection data across the eastern and southern Swiss Alps

Autor(en): **Holliger, Klaus / Kissling, Eduard**

Objekttyp: **Article**

Zeitschrift: **Eclogae Geologicae Helvetiae**

Band (Jahr): **84 (1991)**

Heft 2

PDF erstellt am: **27.09.2024**

Persistenter Link: https://doi.org/10.5169/seals-166780

Eclogae geol. Helv. 84/2: 369–402 (1991)

0012-9402/91/020369–34 $ 1.50 + 0.20/0
Birkhäuser Verlag, Basel

Ray theoretical depth migration: Methodology and application to deep seismic reflection data across the eastern and southern Swiss Alps[1])

By KLAUS HOLLIGER[2, 3]) and EDUARD KISSLING[2])

Key-words: Deep seismic reflection data, migration, Alpine tectonics.

ABSTRACT

Simple analytical considerations show that for the velocities and travel times relevant in deep seismic reflection data, migration displacements easily exceed 5 km vertically and 10 km laterally. This implies that virtually every deep seismic reflection profile needs to be migrated and that a minimum profile length of 30 km is required to allow structural interpretation at lower crustal depths. Estimates of the influence of uncertainties in velocity upon migration show that the error in the average velocity must not exceed 0.2 km/s at Moho depth, in order to allow a meaningful comparison of the reflectivity imaged by normal-incidence profiling and the crustal velocity structure inferred from seismic wide-angle data. Conventional migration schemes based on the solution of the scalar wave equation rarely produce satisfying results when applied to deeper crustal data. A review of the corresponding algorithms shows why these methods are highly sensitive to lateral velocity variations, to the short, laterally discontinuous reflection segments and to characteristics of deep seismic reflection data such as high noise levels in conjunction with the high velocities and long travel times. These problems can be largely overcome by ray theoretical depth migration of digitized line drawings. As a case study the individual deep seismic reflection profiles of the eastern and southern traverses across the Swiss Alps, which were acquired as part of the National Research Program 20 (NFP20), have been combined along the course of the European Geotraverse (EGT). The resulting reflectivity distribution was simultaneously depth migrated with the contours of the smoothed, laterally consistent velocity field obtained by reinterpretation of the seismic wide-angle profiles running parallel to the strike of the Alpine arc. This led to an overall excellent agreement between the most prominent reflectivity patterns and the strongest wide-angle reflections, which is considered to be an important criterion for successful migration. Assuming that the result of this migration represents an unbiased acoustic image of the present-day tectonic configuration of the crust below the central Alps, low angle subduction of the lower crust and upper mantle of the European plate below the Adriatic promontory of the African plate is clearly depicted. Orogenic crustal thickening is interpreted to arise from the stacking of nappes onto the European upper crust and from wedging of the European and Adriatic middle crusts in accordance with existing geological models. At least part of the southvergent upper crustal thrusting in the Southern Alps can be accounted for by the inferred northward downbending of the Moho and lower crust of the Adriatic plate.

---

[1]) Contribution No. 662 Institute of Geophysics, ETH-Zürich.

[2]) Institute of Geophysics, ETH-Hönggerberg, CH–8093 Zürich, Switzerland.

[3]) Now at: Department of Geology and Geophysics, Rice University, P.O. Box 1892, Houston, TX 77251, USA.

ZUSAMMENFASSUNG

Einfache analytische Betrachtungen des Migrationsvorganges zeigen, dass bei den für die kontinentale Kruste relevanten Laufzeiten und Kompressionswellen-Geschwindigkeiten der Migrationsweg 5 km in der vertikalen und 10 km in der horizontalen Richtung oft übersteigt. Einerseits bedeutet dies, dass für eine aussagekräftige Interpretation von reflexionsseismischen Daten deren vorgängige Migration eine *conditio sine qua non* darstellt, und andererseits, dass Profillängen von weniger als 30 km für Untersuchungen der unteren Kruste wenig sinnvoll sind. Ausgehend von analytischen Betrachtungen lässt sich der Einfluss von Fehlern in der Parametrisierung des Geschwindigkeitsfeldes auf den Migrationsweg abschätzen. Dabei ergibt sich, dass für einen aussagekräftigen Vergleich zwischen der aus refraktionsseismischen Daten abgeleiteten Geschwindigkeitsstruktur und der durch die Migration erhaltenen Reflektivitätsverteilung die Unsicherheit in der mittleren Krustengeschwindigkeit einen Wert von 0,2 km/s nicht überschreiten sollte. Die gängigen, vornehmlich von der Erdölindustrie entwickelten Migrationsverfahren basieren auf der numerischen Lösung der skalaren Wellengleichung für die Rand- und Anfangswerte der gemessenen seismischen Daten. Derartige Migrationsalgorithmen reagieren sowohl sensibel auf laterale Änderungen der Geschwindigkeit wie auch auf Unzulänglichkeiten in den Anfangs- und Randbedingungen, wie z.B. geringes Verhältnis von Nutz- zu Störsignal und unvollständige Registrierung des reflektierten Wellenfeldes. Ausserdem lässt sich zeigen, dass mit der Genauigkeit eines solchen Migrationsalgorithmus in Bezug auf die Lösung der skalaren Wellengleichung auch dessen Empfindlichkeit gegenüber den obengenannten Phänomenen zunimmt. Damit lassen sich einerseits die wohlbekannten Probleme bei der Migration von krustenseismischen Reflexionsdaten erklären, und andererseits wird klar, dass wenig Hoffnung besteht, ausgehend von der Wellentheorie Algorithmen zu entwikkeln, welche diese Probleme grundsätzlich lösen. Die Migration der beobachteten Laufzeiten basierend auf der geometrischen Strahltheorie, einer Hochfrequenzapproximation der Wellentheorie, stellt daher zur Zeit und wohl auch in absehbarer Zukunft für krustenseismische Reflexionsdaten die praktikabelste Lösung dar. Als Fallstudie wurden die Reflexionsprofile der Ost- und Südtraverse des Nationalen Forschungsprogramms 20 (NFP 20) «Geologische Tiefenstruktur der Schweiz» betrachtet. Diese Reflexionsprofile wurden entlang des alpinen Segments der Europäischen Geotraverse (EGT) kombiniert und anschliessend strahlentheoretisch tiefenmigriert. Die für die Migration benötigte Geschwindigkeitsinformation ergab sich durch eine lateral geglättete Reinterpretation der parallel zum alpinen Streichen verlaufenden Refraktionsprofile. Diese Migration führte zu einer generell guten Übereinstimmung zwischen den dominierenden Reflektivitätsmustern und den über den gesamten Zentralalpenbogen hinweg lateral kontinuierlich verfolgbaren Weitwinkelreflexionen. Das resultierende akustische Bild der Erdkruste unter den Zentralalpen reicht in eine Tiefe von 60 km und weist unter anderem mit einer mit etwa 15 Grad nach Süden geneigten Moho auf die Subduktion der untersten Kruste der europäischen unter die afrikanische Platte hin. Die orogene Verdickung der alpinen Kruste lässt sich einerseits durch die Stapelung von Kristallindecken in der Oberkruste der europäischen Platte und andererseits durch ein Ineinanderschieben der Mittelkrusten der europäischen und afrikanischen Platten interpretieren. Das nordvergente Abtauchen der Unterkruste der afrikanischen Platte kann die beobachtete südvergente Verkürzung der Oberkruste in den Südalpen zumindest teilweise erklären.

Introduction

The first normal incidence reflections from within the crystalline basement were observed and identified by Junger (1951) during conventional seismic reflection prospecting for oil in Montana. In the following years more and more similar observations were made particularly by German seismologists (see Dohr & Meissner 1975 for a review) normally just by extending the recording time during routine seismic reflection work. By the mid-seventies the observational success of these pioneering efforts eventually led to the establishment of reflection seismology as a scientific tool to explore the fine structure of the lithosphere (cf. Brown 1986).

The basic philosophy of deep seismic reflection profiling is identical to that used in two-dimensional seismic exploration (see e.g. Robinson 1983 or Schneider 1984 for a comprehensive review). To achieve a redundant imaging of the subsurface, seismic data are acquired by continuously moving the source and the receiver array along the profile. Assuming plane horizontal layering of the subsurface, the data are then rear-

ranged according to common source-receiver midpoints, commonly referred to as common midpoints (CMPs) or – semantically less correct – common depth points (CDPs) or common reflection points (CRPs). It can be shown that seismic reflections in the CMP-domain show a quasi-hyperbolic dependence of travel time versus offset even if these reflections arise from dipping interfaces. The so-called normal moveout (NMO) correction aims at flattening these reflection hyperbolae so that subsequent summing or "stacking" of all the NMO-corrected traces of a CMP-gather results in one single trace with a statistically improved signal-to-noise ratio (S/N). The set of all summed CMP-traces represents the final stacked seismic section, which ideally is zero-offset. The surface location of each trace may then be thought of as a coincident source and receiver position and hence the trace only contains seismic energy which has travelled the same way down from the source to a reflector and up again to the receiver. In this case the wave front vector must be perpendicular to each reflector and therefore no reflected shear waves are excited. In the following it is assumed that no shear waves are present and hence, whenever we mention seismic velocity, we always refer to the velocity of compressional waves.

As is evident from the "layer cake" assumption upon which the CMP-concept is based, reflection seismology was originally designed to image relatively simple geologic structures in sedimentary basins and hence the early reports of seismic reflections from within the crystalline basement were a big surprise to most experts. Even today it is far from obvious what in detail gives rise to the strong reflected signals from the lower and middle crust (cf. Warner 1990a). The NMO-correction becomes almost negligibly small at middle and lower crustal levels, and thus smoothes out many of the complexities along the wave path. This, as well as the evidently high impedance contrasts (Warner 1990b), contribute most substantially to the successful imaging of crustal reflectors.

Acquisition and processing of deep seismic reflection data including S/N enhancement, NMO-correction and CMP-stack have reached a high degree of maturity and standardisation (Brown 1986; Warner 1986; Klemperer 1989). This is not the case for the so-called migration of deep seismic reflection data which aims at removing the distortions introduced by the CMP-concept in order to allow a geologic interpretation of the data. In the first part of this paper we wish to give the interpreting geologist a flavour of the basic concept and the relevance of the migration process and we present a migration method which we consider to be particularly well suited for deep data. In the second part we apply this method to deep seismic reflection profiles across the eastern and southern Swiss Alps which were acquired as part of the National Research Program 20 (NFP20) "Geologische Tiefenstruktur der Schweiz" (Frei et al. 1989).

Migration

Basic Geometric Considerations

Figure 1 illustrates the geometric effect of migration upon a zero-offset, i.e., CMP-stacked seismic section for a medium of constant velocity. Due to the assumption of plane horizontal layering of the subsurface inherent in the CMP-concept, a dipping reflection is plotted vertically below the coincident source and receiver location. How-

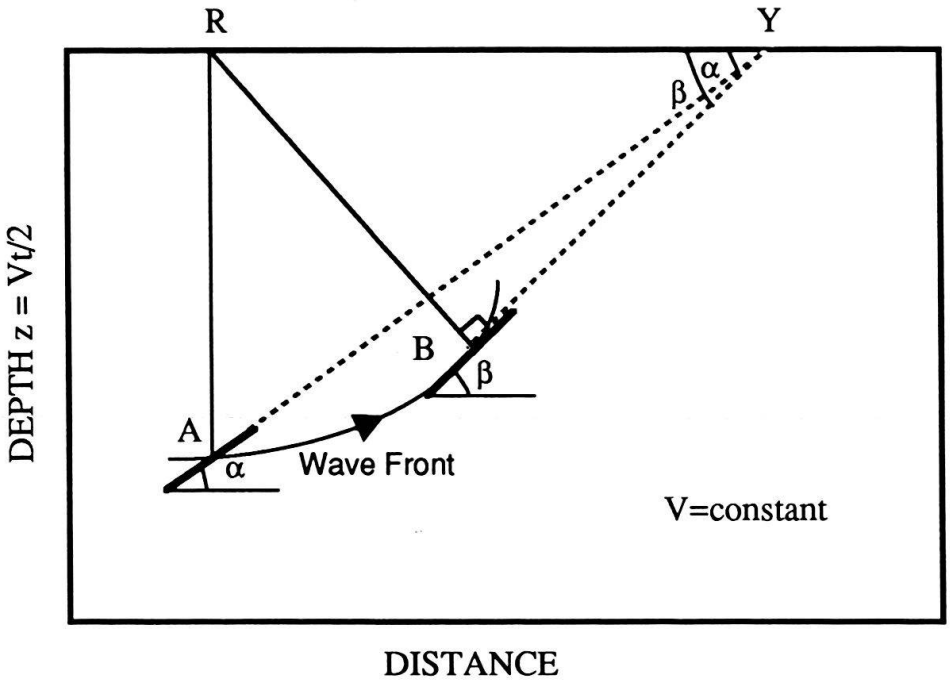

Fig. 1. Schematic illustration of the geometry of the migration process in a homogeneous medium. Vertical axis is depth but, due to the constant velocity, may be considered as scaled travel time. Before migration, the line element A dips at an apparent angle α and is located vertically beneath the coincident source/receiver location R on the stacked, zero-offset section; migration moves the element updip to position B where it dips at the true angle β and is parallel to the wave front, i.e. perpendicular to the incident ray.

ever, elementary geometric considerations show that this cannot be the true spatial position of a dipping reflector since the incident seismic energy would not travel the same way up again after reflection and hence not reach the receiver. To satisfy the zero-offset concept the reflector has to be moved updip along the wave front until it is perpendicular to the incident ray (Fig. 1). This process is referred to as migration, or less commonly – albeit semantically more correct – as seismic imaging, seismic image reconstruction, wave field reconstruction, wave field extrapolation or wave field depropagation.

It is easy to see from Figure 1 that the apparent dip α of the unmigrated reflector is related to the true dip β of the migrated reflector by

$$\tan \alpha = \sin \beta \tag{1}$$

Two fundamental lessons can be learnt from this very simple relationship:

- The apparent dip must not exceed 45 degrees. Any steeper dips in the unmigrated seismic section necessarily represent artefacts, such as effects from the third dimension.
- The true dip of a reflector after migration is always bigger than its apparent dip before migration, i.e., migration increases the dip by moving the reflector updip along the wave front.

Formula (1) may be extended to establish the relationship between the unmigrated (X_{unmig}, Z_{unmig}) and the migrated position (X_{mig}, Z_{mig}) of a reflector (Chun & Jacewitz 1981):

$$X_{mig} = X_{unmig} + \frac{v^2 t \tan \Phi_t}{4}$$
$$Z_{mig} = Z_{unmig} + \frac{v}{2} t \left\{ 1 - \sqrt{1 - \frac{v^2 \tan^2 \Phi_t}{4}} \right\} \quad (2)$$

where v is the constant velocity of the medium, t the observed reflection time and

$$\tan \Phi_t = \frac{\Delta t}{\Delta x} = 2 \frac{\tan \alpha}{v}$$

The interpreting geologist may find (2) useful to achieve a first guess on the spatial position and hence of the possible structural significance of the individual reflections from an unmigrated seismic section. Figure 2 shows the thus calculated horizontal and vertical displacements for a range of apparent dip angles as a function of reflection time. The velocity is taken to be 6.0 km/s which is a representative average value for crustal studies. It becomes evident that for the travel times and apparent dips relevant for deep seismic reflection data migration paths down to middle and lower crustal levels easily exceed 5 km vertically and 10 km horizontally. This implies that virtually every deep reflection profile needs to be migrated in order to make it accessible to tectonic interpretation. These results also imply that in structurally complicated areas deep seismic reflection profiles should have a minimum length of some 30 km; otherwise the interpretation is prone to be biased since not only a lot of information will migrate out of the profile but also a lot of information that should migrate into the profile will be lacking.

The convergence of migrated reflectivity patterns with interfaces of the large-scale velocity structure of the crust determined by seismic wide-angle profiles (Ansorge 1989) is not only a possible criterion for a successful migration but also a key to a better understanding of the origins of crustal reflections. It is therefore relevant to have a feeling of how sensitive the migration process is with respect to uncertainties in velocity. This may be achieved by differentiating (2) with respect to the velocity v. Figure 3 shows the migration errors resulting from a velocity uncertainty of ± 0.2 km/s with respect to a uniform background velocity of 6.0 km/s. Mispositioning – particularly in the vertical direction – becomes substantial even for moderate apparent dips around 20 degrees and travel times around 5 s. Hence every effort must be made to determine the average velocity structure used for migration as precisely as possible, certainly within ± 0.2 km/s or even better. In crustal studies this accuracy can only be achieved by seismic wide-angle data. Experience from workshops (cf. Ansorge et al. 1982) in fact shows that – despite often considerable differences in the details of the crustal velocity structure – the average crustal velocities and crustal thickness, independently inferred by different workers from good quality seismic wide-angle data, agree within 0.1 to 0.2 km/s and 2 km, respectively.

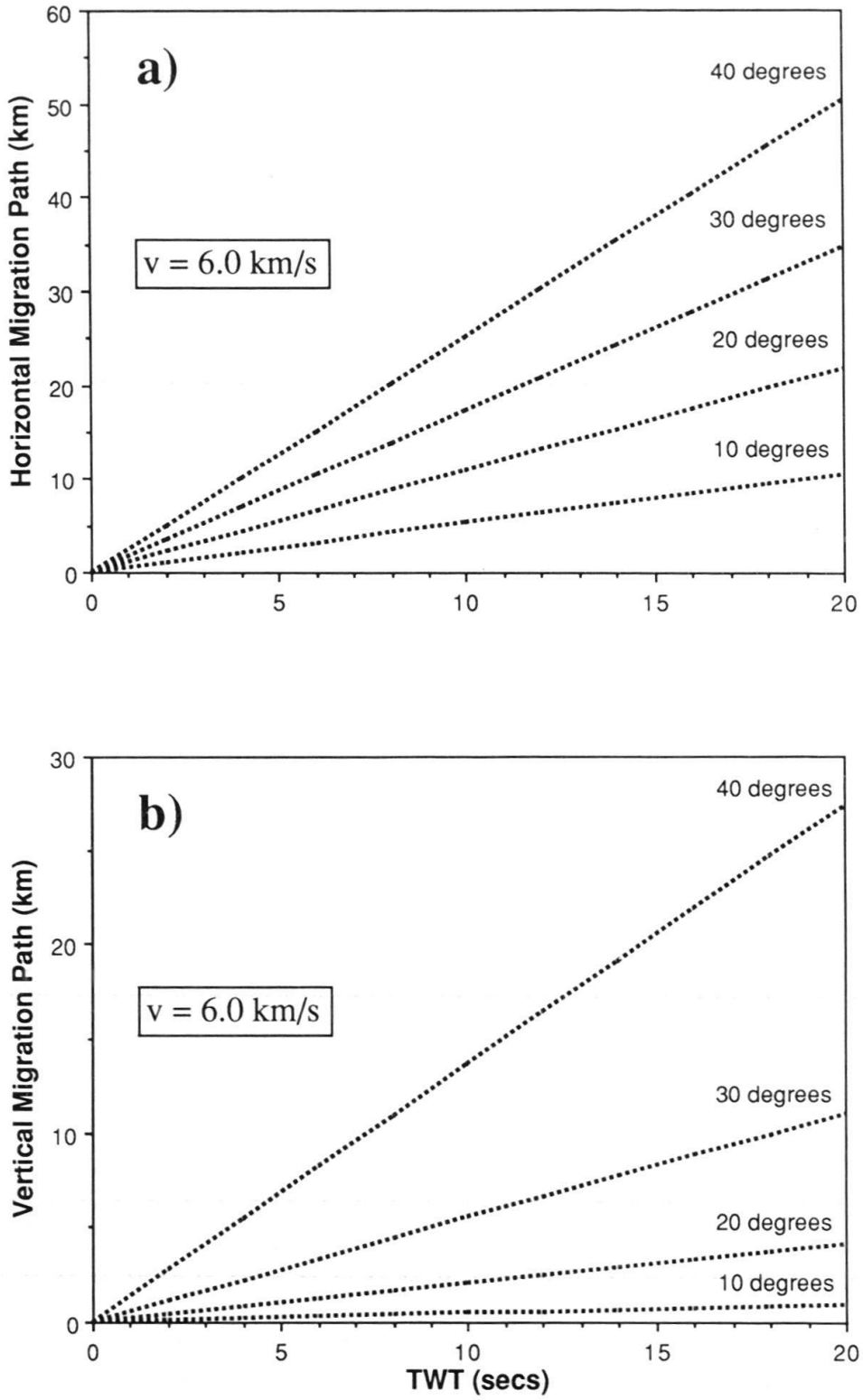

Fig. 2. Horizontal (a) and vertical (b) migration displacements as a function of apparent reflector dip and travel time. The velocity of the overburden is taken to be constant at 6.0 km/s, which is a representative average value for crustal studies.

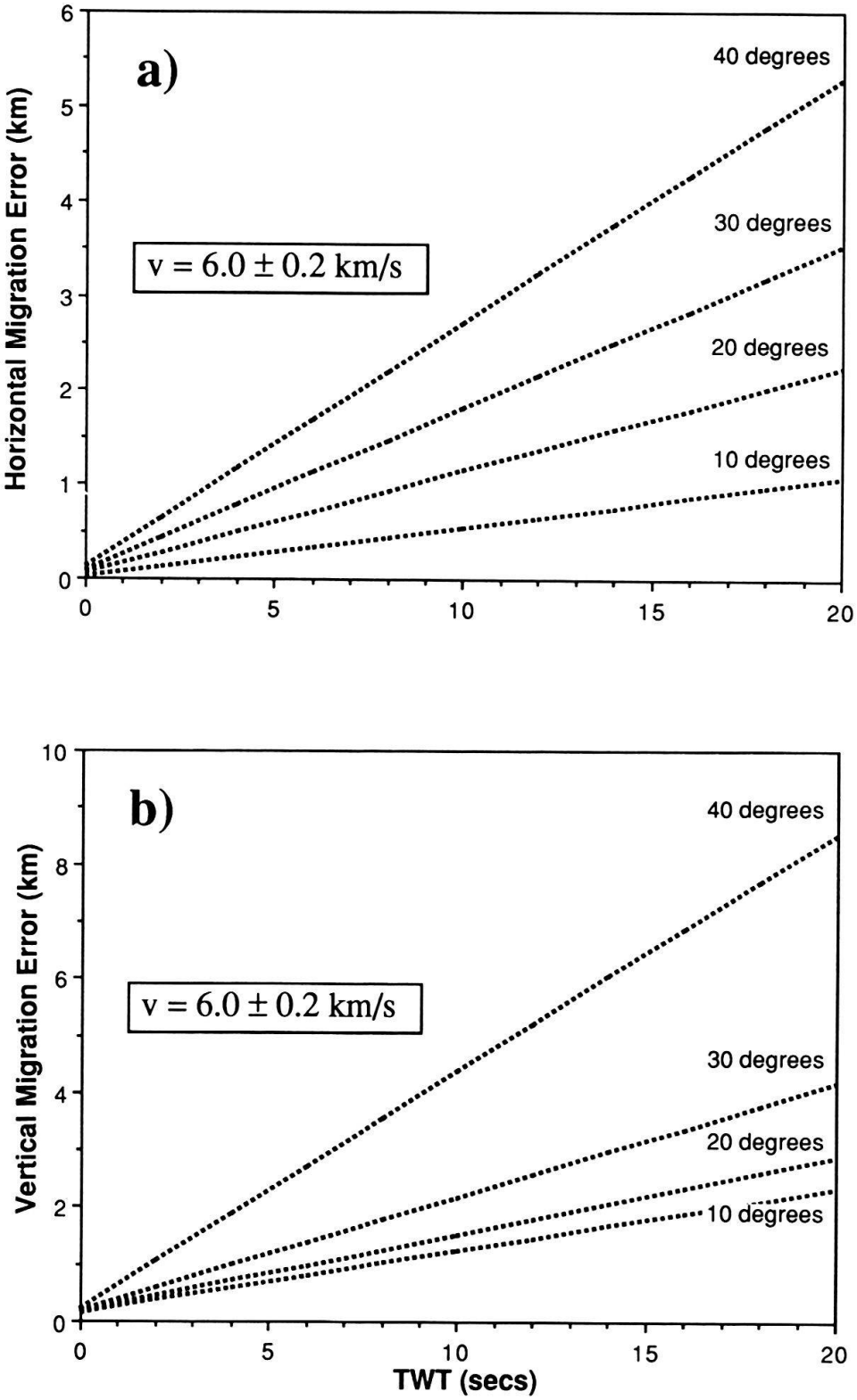

Fig. 3. Horizontal (a) and vertical (b) migration errors as a function of apparent reflector dip and travel time for an uncertainty in velocity of 0.2 km/s relative to 6.0 km/s.

So far we have just considered media of constant seismic velocity for which the ray paths indicating the direction along which the seismic energy travels are straight. Geologically more realistic media, however, require lateral and vertical variations of seismic velocity, which results in a bending of the ray paths. These bending effects have so far been neglected and therefore the above estimates of the migration path and migration error represent minimum values. In the following we shall first briefly review the problems of conventional migration schemes with respect to deep data and then show how geometric ray theory can be used to accurately migrate line drawings of seismic reflection through complex velocity structures.

Wave Equation Migration

Standard migration procedures developed and used by the oil industry take the stacked seismic data as the boundary/initial condition to some numerical solution of the acoustic wave equation, which aims at depropagating the observed wave field through the long wave length part of the velocity structure to unravel its short wave length part, i.e., the reflectivity of the subsurface (cf. GAZDAG & SGUAZZERO 1984). Ideally this so-called wave equation migration not only repositions the data correctly and preserves their original character (i.e., amplitude and phase attributes) but also increases the spatial resolution by removing the effects of the geometric spreading of the propagating wave front.

Wave equation migration works well provided that the S/N is high, the velocity structure is simple and well known and the wave field is fully sampled. Virtually all of these prerequisites are commonly violated by deep seismic reflection data: the S/N is notoriously low, often very low, the velocity structure is rarely simple and often poorly constrained and due to complexities of the overburden the reflected wave field cannot be expected to be sampled completely. For high velocities and/or long travel times migration has the same effect as the so-called trace mixing, which enhances the low wave numbers, thus giving the data a smeared and "wormy" look. Incomplete sampling of the reflected wave field is indicated by the lateral discontinuity of crustal reflectors and the absence of diffractions at the edges of the reflectors. Wave equation migration nevertheless compensates for these "missing" diffractions, which results in a smiley look of the migrated data (WARNER 1987). Attempts to overcome at least the noise problem by harsh enhancement of coherent energy either before (e.g. VALASEK et al. 1990) or during (MILKEREIT 1987) migration have led to certain improvements. However, a sensitive parametrisation of the coherency filter and the gain function results in the loss of much of the original amplitude and phase information and makes this approach prone to the introduction of artefacts. Since unstacked and stacked deep seismic reflection data bear essentially the same characteristics the above considerations also apply to the migration of unstacked data, the so-called pre-stack migration.

The above data insufficiencies represent fundamental violations of the boundary/initial value problem upon which wave equation migration is based and therefore their disastrous effect increases with the accuracy required of the migration algorithms. As a consequence, conventional wave equation of deep seismic reflection data is – and will remain – inherently problematic.

Ray Migration

Geometric ray theory represents an asymptotic approximation of wave theory for the case of infinitely high frequencies. As such it explicitly excludes any frequency dependent effects such as diffractions, interference and dispersion, but it is able to correctly predict the travel time of seismic waves through relatively complex media (e.g. RAYNAUD 1988a). In two dimensions the propagation of rays is governed by the following system of ordinary linear differential equations of the first order (e.g. ZELT & ELLIS 1988)

$$\begin{aligned} \frac{dx(t)}{dt} &= v(x,z) \cdot \sin\theta \\ \frac{dz(t)}{dt} &= v(x,z) \cdot \cos\theta \\ \frac{d\theta(t)}{dt} &= -\frac{dv(x,z)}{dx} \cdot \cos\theta + \frac{dv(x,z)}{dz} \cdot \sin\theta \end{aligned} \tag{3}$$

where v (x, z) is the velocity at a particular point, t the travel time and θ the ray's angle to the vertical. A particular ray is uniquely defined by its initial conditions, which have to be updated according to Snell's law whenever the ray hits a velocity interface. This makes ray theory a well behaved kinematic tool for migration, since – unlike wave equation migration – it will only do what one tells it to, nothing more but also nothing less (RAYNAUD 1988b). In order to use geometric ray theory for migration, one first has to prepare a digital line drawing of the original seismic data and then work out the initial conditions for the integration of system (3).

In terms of filter theory the process of line drawing preparation may be described as a convolution of the original seismic data, consisting of amplitude, phase and corresponding travel time information as well as noise, with the coherency filter of the human eye and mind. Ideally this filtering process would result in a noise-free copy of the original seismic data, consisting of the travel times of all the primary reflections and diffractions, with the amplitude and phase information removed. Undoubtedly manual line drawing preparation (PFIFFNER et al. 1990b) is a subjective and at this stage an undesired interpretational process since it depends on the preconception of the individual workers. On the other hand computer-generated line drawings (VALASEK et al. 1990) are subjective as well due to sensitive parametrisation of the coherency filter. It is of course not possible to quantify the accuracy of a line drawing, but experience has shown that – despite often substantially different interpretative approaches – line drawings independently made by different workers generally agree amazingly well in terms of their overall character and major reflectors (compare e.g. GIBBS (1987) with HOLLIGER & KLEMPERER (1989) or FREI et al. (1989) with Figures 8a, b, c, d).

The most important prerequisite for reducing the ambiguity inherent in line drawing preparation is to start with carefully processed seismic data, which not only has an optimized signal to noise ratio but also may be expected to be largely free of non-primary coherent energy. Should it not be possible to remove all the non-primary coherent energy – such as multiples and side-swipe – in the processing stage, this may be done in an interpretative way during line drawing preparation (HOLLIGER & KLEM-

PERER 1989). A question that remains open for debate is whether line drawing preparation should be accompanied by any further subjective optical filtering, such as rejecting coherent energy below a certain spatial extent (manual spatial deconvolution) or removing the reverberating character typical of many crustal reflections (manual vertical deconvolution). Assuming that a good job has been done in the processing stage, all coherent energy must be considered as being part of the reflectivity of the subsurface, which we are looking for. Since RAYNAUD (1988b) has shown that corresponding travel times are correctly predicted by ray theory even in the presence of complex overburden, we advocate the inclusion of all clearly coherent events in the original line drawing. Additional filtering based on length, dip, bending or "amplitude", may still be performed numerically on the digital line drawing before and/or after migration. Practical problems concerning line drawing preparation are discussed in HOLLIGER & KLEMPERER (1989); VALASEK & HOLLIGER (1990) and WARNER (1986, 1987) and are illustrated in Figure 6 on the example of the northernmost 15 km of the NFP20 eastern traverse. In the following a digitized line drawing of an individual reflection or diffraction is called a *reflection segment.* Each reflection segment is defined by N points with $N \geq 2$. Thus a reflection segment is made up of N-1 *line elements* each of which is defined by its two endpoints.

As illustrated by Figure 1 the problem consists of shifting each line element updip along the corresponding wave front until it is perpendicular to the incident ray. The geometric construction of the reflection point is the inverse of that used to produce a synthetic zero-offset section by inverse ray tracing (TANER et al. 1970). For a given two-dimensional velocity model the location of the reflection point is thus uniquely defined by this construction. The problem, hence, is to define the correct initial conditions for this inverse normal incidence ray tracing procedure. As mentioned above, the initial conditions required for ray tracing are the coordinates of the starting point and the initial angle of the ray. The former is given as the surface location of the unmigrated reflection point; the latter requires the knowledge of the starting angle of the normal incidence ray and has to be determined separately for each line element.

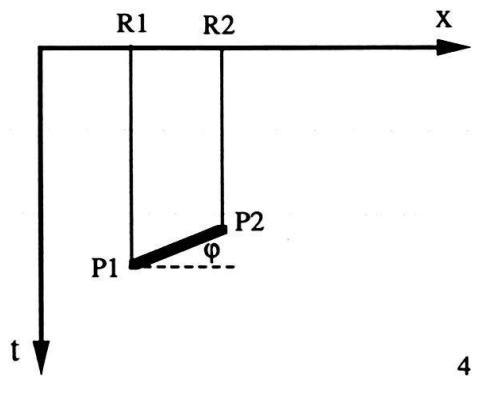

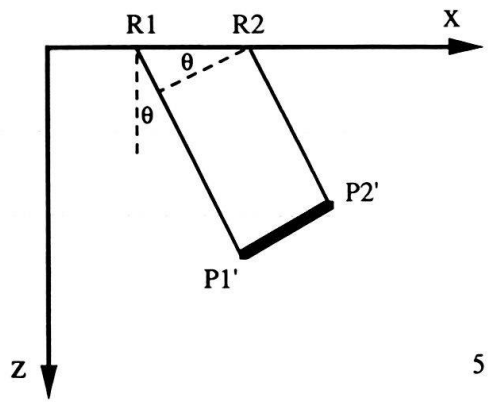

Fig. 4. Unmigrated line element defined by its end points P1 and P2 lying vertically below the corresponding coincident source/receiver locations R1 and R2. Vertical axis is travel time, which is assumed to be scaled according to the "effective velocity" relevant for this line element.

Fig. 5. Line element of Figure 4 after ray theoretical depth migration.

Figure 4 shows an unmigrated line element defined by two points P_1 (x_1, t_1) and P_2 (x_2, t_2). The vertical axis is travel time and is assumed to be scaled according to the so-called effective velocity v_{eff} which corresponds to the average velocity along the corresponding normal incidence ray and is defined as

$$v_{eff} = \frac{\int_S v(s)\, ds}{S} \tag{4}$$

where S represents the total length of the ray path. The apparent dip φ is given by

$$\tan \varphi = \frac{v_{eff}}{2} \frac{\Delta t}{\Delta x} \tag{5}$$

where $\Delta x = x_2 - x_1$ and $\Delta t = t_2 - t_1$. As evident from Figure 5, which shows the same line element after depth migration, the starting angle θ for a particular ray element is determined by the length difference of the two normal incidence rays. Therefore

$$\sin \theta = \frac{v_o \tan \varphi}{v_{eff}} \tag{6}$$

where v_o is the velocity immediately below the corresponding source/receiver pair. This concept is only valid if v_{eff} is the same for both rays. Experience shows that this condition is virtually always fulfilled if the velocity model is sufficiently smooth for ray tracing and if the individual line elements are not too long. Otherwise this condition can easily be checked and the problem can be removed either by discarding the line element, chopping it up into several shorter elements or by slightly changing the crucial parts of the velocity structure.

If the profile is at angle ζ to the dip direction Δx in (5) has to be replaced by $\Delta x'$, which is defined as (e.g. Levin 1971)

$$\Delta x' = \Delta x \cos \zeta \tag{7}$$

Correspondingly the effect of uniform axial plunge Φ can be accounted for by

$$\Delta t' = \Delta t / \cos \Phi \tag{8}$$

Corrections (7) and (8) are linear and may therefore be combined. They allow to remove undesired effects from the third dimension provided these effects are the same for imaged geological structures.

Knowing the initial conditions of the ray tracing system, the migration procedure for an individual reflection segment can now be outlined as follows (see Appendix for details):

(1) Determine the starting angle for the first line element.

(2) For each of the two points defining the line element, trace one ray through the medium. The rays obey the ray equations and Snell's law at interfaces. Ray tracing for a point is finished when the ray has travelled for half the observed travel time of this

point. If the rays are not perpendicular to the line element the velocity structure of the particular area is smoothed and the procedure is reset to (1).

(3) Repeat (1) and (2) for all the remaining line elements of the reflection segment.

(4) The depth migrated reflection segment is defined by joining the individually depth migrated line elements.

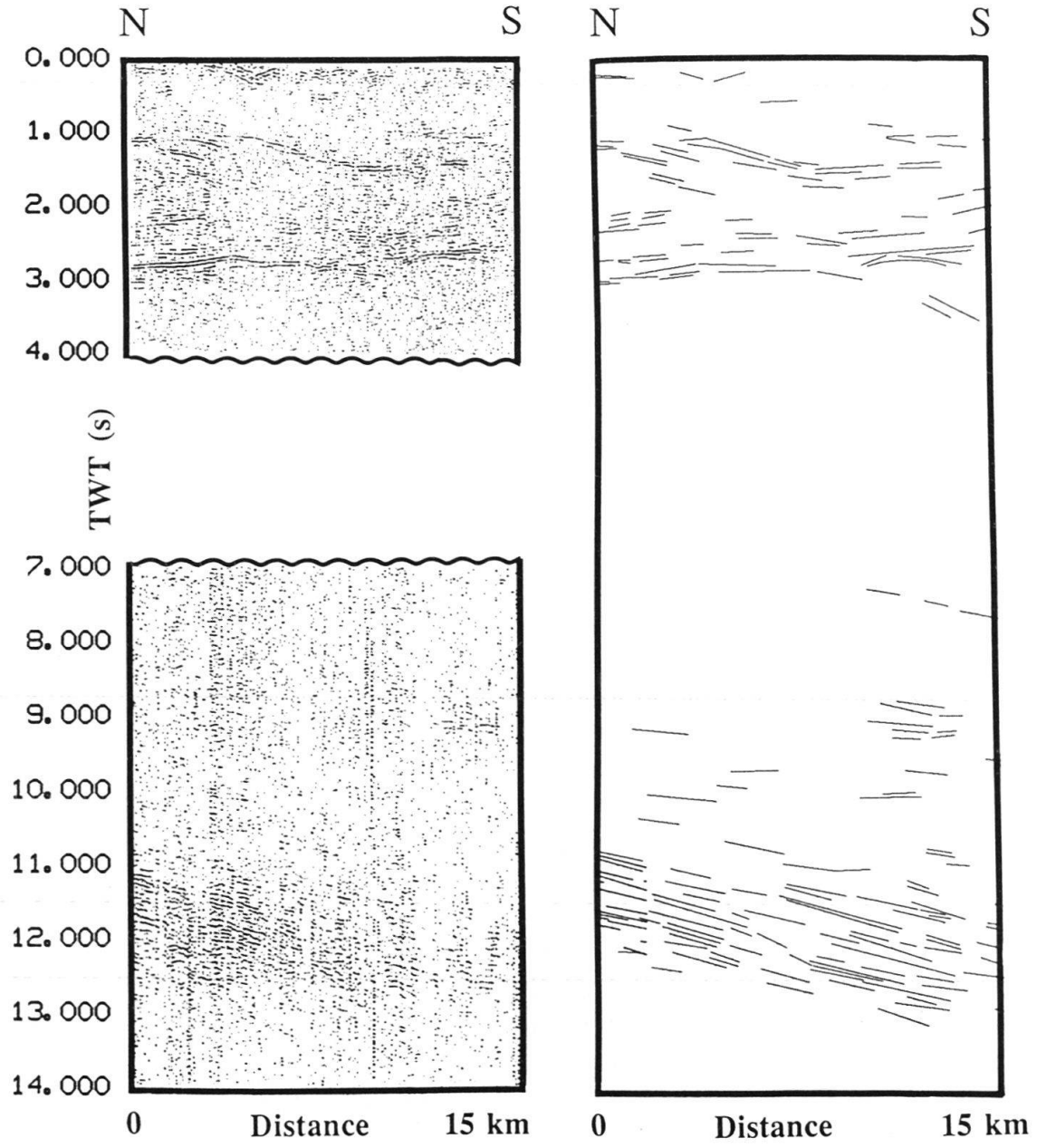

Fig. 6. Illustration of the line drawing preparation process on the northernmost 15 km of the NFP20 eastern traverse (see also text). Horizontal and vertical scales are approximately 1:1 for an average crustal velocity of 6.0 km/s. Top left: Topmost 4 s travel time of the processed, multifold Vibroseis data used for line drawing preparation in the upper crust. Bottom left: 7 to 14 s travel time processed, single fold dynamite data used for line drawing preparation in the middle and lower crust. Right: line drawing derived from the seismic data on the left-hand side.

The thus defined migration procedure is equivalent to the wave front migration method of HAGEDOORN (1954) which not only correctly repositions reflections but also "collapses" diffractions by moving the individual line elements into the apex. Moreover, the change in length of a line element due to migration is indicative of focusing and defocusing effects of the overburden and may be used to calculate "ray migration amplitudes" (RAYNAUD 1988b). These focusing and defocusing effects predicted by ray theory are, however, not to be confused with the shrinking of the Fresnel zone and the increase in spatial resolution achieved by wave equation migration (cf. BERKHOUT & VAN WULFFTEN PALTHE 1979; LINDSEY 1989). For the case of constant layer velocities ray theory optionally allows to migrate the velocity structure as well. This can be done by either directly defining the velocity model in travel time or by converting it from depth to travel time along vertical ray paths. The interfaces of this "time model" are chopped up into smaller segments in order to fulfil (6), then converted into the line drawing format described above and, lastly, migrated in the same way as reflection segments. The simultaneous depth migration of the structural model of the subsurface and the observed reflectivity can be useful for interpretative migration. Convergence of the migrated reflections and the geometry of the velocity structure is a possible criterion for the correctness of the latter. Algorithmic details of the above ray migration procedure are given in the Appendix.

Deep Seismic Reflection Profiles of the NFP20 Eastern and Southern Traverses

Deep Seismic Reflection Data

Figure 7 shows a schematic tectonic map of Switzerland with the seismic reflection profiles of the NFP20 eastern and southern traverses (FREI et al. 1989) as well as the major seismic wide-angle profiles superimposed. The ultimate goal of the NFP20 deep seismic reflection profiling campaign was to obtain a detailed unified acoustic image of the crust below the central Alps by a series of traverses. The easternmost is subparallel to the Alpine segment of the European Geotraverse (EGT) (cf. MUELLER & BANDA 1983). Logistic problems did not allow to shoot this Alpine reflection traverse in the form of one single profile. Rather the traverse consists of four seismic reflection profiles (ET, S1, S3, S5) crossing the entire arc of the central Alps from the Subalpine Molasse in the north to the edge of the Po Basin in the south (Fig. 7). The individual profiles range in length from 5 (line S5) to 95 km (line ET). The problem to be solved is therefore not only the imaging process *sensu strictu,* i.e., the depth migration of the observed reflectivity, but also the combination of the individual seismic lines into one single profile.

The acquisition and processing strategies applied to the NFP20 deep seismic reflection data have been discussed in detail by VALASEK et al. (1990) and PFIFFNER et al. (1990a) and consequently only those aspects relevant to line drawing preparation are recapitulated here.

The entire eastern traverse (line ET) and line S3 of the southern traverse were acquired using both Vibroseis and explosive sources. The Vibroseis source has a controlled source spectrum and provides a high resolution at upper crustal levels (down to approximately 5 s travel time) but, at the high ambient noise levels common in Switzer-

land, generally fails to penetrate sufficiently the deeper parts of the crust. This energy deficiency at lower crustal levels was compensated by detonating strong but loosely spaced explosive charges into the same receiver spreads (charge sizes vary roughly between 100 and 1,000 kg; shot spacing is approximately 10 km on average).

In order to portray the reflectivity in the subsurface of lines ET and S3 as accurately as possible, the line drawings were prepared from the Vibroseis data in the upper part and from the dynamite data in the lower part. While combining the two datasets during line drawing preparation, i.e., Vibroseis data for the upper and middle crust and dynamite data for the middle and lower crust, we generally found – despite the crooked line geometry and the relatively large offsets of the dynamite data – a good

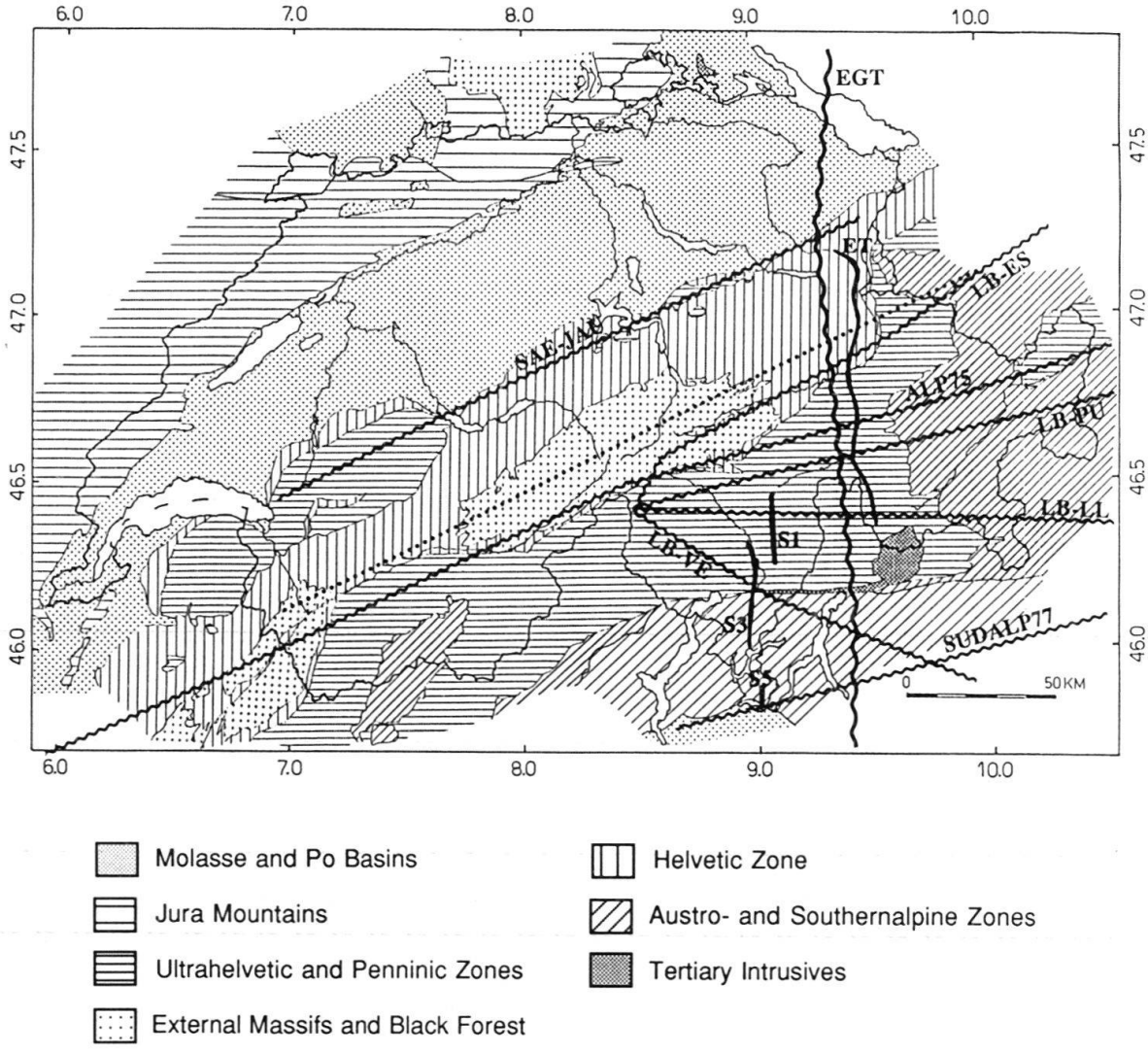

Fig. 7. Schematic tectonic map of Switzerland with the location of the seismic wide-angle (wavy lines) and normal-incidence reflection profiles (solid lines) superimposed. The dotted line represents the Aar Massif profile shot in 1988, which is not yet interpreted. The numbers outside the frame denote latitude and longitude in degrees. EGT: European Geotraverse, SAE-JAU: Säntis-Jaunpass, LB-ES: Lago Bianco-Eschenlohe, ALP75: Alpine Longitudinal Profile, LB-PU: Lago Bianco-Pustertal, LB-LL: Lago Bianco-Lago Lagorai, LB-VE: Lago Bianco-Verona, SUDALP77: Southern Alps profile, ET: NFP20 Eastern Traverse, S1, S3, S5: NFP20 Southern Traverse lines 1, 3 and 5.

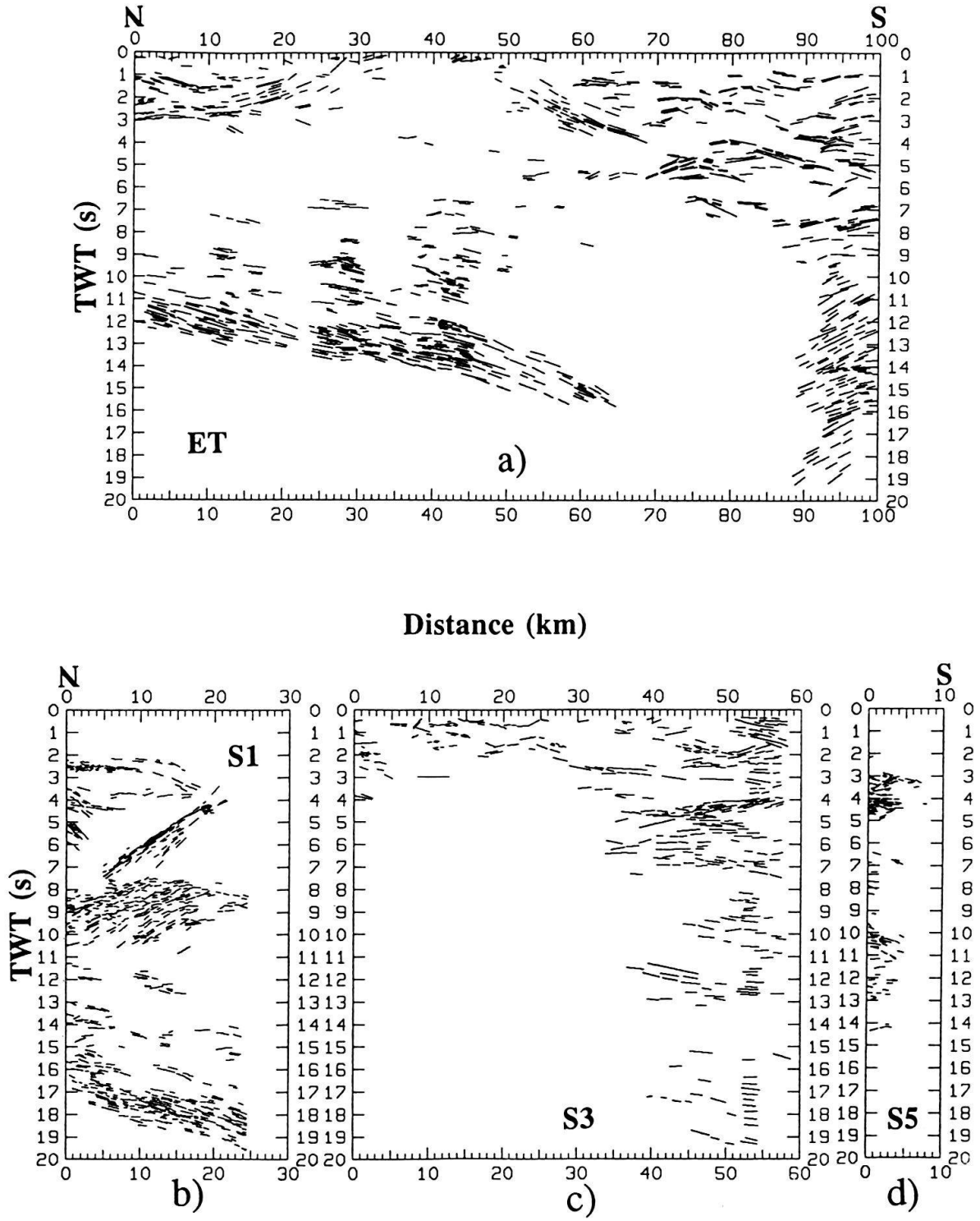

Fig. 8. Unmigrated digitized line drawings prepared from the NFP20 eastern and southern traverses. Horizontal (distance in km) and vertical (travel time in s) scales are 1:1 for an average crustal velocity of 6.0 km/s. For location see Figure 7.

a) Unmigrated line drawing of line ET (Vibroseis and dynamite combined)

b) Unmigrated line drawing of line S1 (dynamite only)

c) Unmigrated line drawing of line S3 (Vibroseis and dynamite combined)

d) Unmigrated line drawing of line S5 (dynamite only)

correlation of reflectors that were imaged by both datasets, i.e., in middle crustal level. The most likely explanation for this phenomenon is a considerable lateral continuity of the most prominent reflectors. In contrast to lines ET and S3, lines S1 and S5 were acquired using loosely spaced explosions only and consequently their resolution in the topmost 2 to 3 s travel time is much lower than the one of the lines ET and S3. Every effort was made to conserve as much as possible of the internal characteristics of the various reflectivity patterns observed in the different tectonic units (Valasek et al. 1991). Figures 8a, b, c and d show the unmigrated line drawings digitized from lines ET, S1, S3 and S5.

Migration Velocity Model

Unlike stacking velocities, migration velocities have a true physical meaning in that they represent the large scale velocity structure of the medium. The migration procedure depropagates the observed wave field (the unmigrated time section) through this large scale velocity structure in order to obtain an undistorted acoustic image of the reflectivity (i.e., the small scale variations of the velocity field) of the subsurface geology. Seismic wide-angle profiles represent the only means to provide this velocity information with the required accuracy on a crustal scale (Ansorge 1989).

Whilst in areas where lateral tectonic variations are less dramatic than in the Alps coincident parallel seismic reflection and spatially loosely sampled wide-angle profiles may be an ideal combination (Mooney & Brocher 1987), in more complicated environments seismic wide-angle profiles ought to be oriented parallel to the structural trend in order to reduce the negative effects of spatial aliasing upon lateral resolution. On the other hand seismic reflection profiles are best oriented perpendicular to the tectonic trend in order to permit an unbiased and complete sampling of a two-dimensional cross section through the actual three-dimensional wave field. Therefore the availability of densely spaced (approximately 20 km on average) seismic wide-angle profiles oriented parallel to the structural grain of the central Alpine arc (Fig. 7), which is the result of long-term careful scientific planing and coordination at an international level (cf. Mueller et al. 1980 and references therein), to our knowledge represents an unique situation.

The migration velocity model for the combined NFP20 deep seismic reflection profiles was derived by reinterpreting the main features of these profiles and combining the resulting one-dimensional velocity-depth functions along the EGT. The velocity structure was kept as simple as possible, i.e., no velocity gradients or dipping interfaces were introduced unless explicitly required by the data. This so-called minimum interpretation (Holliger 1991) of the individual seismic wide-angle profiles was achieved by first deriving an approximate one-dimensional velocity-depth function by Wiechert-Herglotz inversion and X^2–T^2 analysis and subsequent verification and refinement by forward ray tracing.

Since such an approach strongly emphasizes lateral continuity, locally clear but laterally discontinuous wave groups were discarded in some places, whereas in other places weak but otherwise laterally continuous wave groups were considered. The travel time correlations of the selected wave groups were adopted from previous interpretations (Egloff 1979; Deichmann et al. 1986; Maurer 1989; Yan & Mechie

1989). All seismic wide-angle profiles relevant to this study intersect the EGT and with the exception of the Säntis-Jaunpass profile, all of them image the entire crust below the EGT. Therefore, the migration velocity model can be constructed without projection (again with the exception of the Säntis-Jaunpass profile) directly from the velocity-depth functions of seismic wide-angle profiles at their intersection points with the EGT. Lateral velocity variations turned out to be rather mild on a large scale. Therefore, a migration velocity model with the following constant interval velocities was considered to be appropriate:

- Sediments (Subalpine Molasse, Southern Alps): 5.0 km/s (Stäuble 1990; Deichmann et al. 1986).
- Upper crust: 6.1 km/s
- Lower crust: 6.5 km/s
- Upper mantle: 8.1 km/s.

The geometry of the base of the sediments of the Subalpine Molasse and the Southern Alps was inferred directly from the unmigrated seismic reflection data. By no means is the resulting velocity model shown in Figure 9 intended to be an alternative or an improvement on any previous (Egloff 1979; Deichmann et al. 1986; Maurer

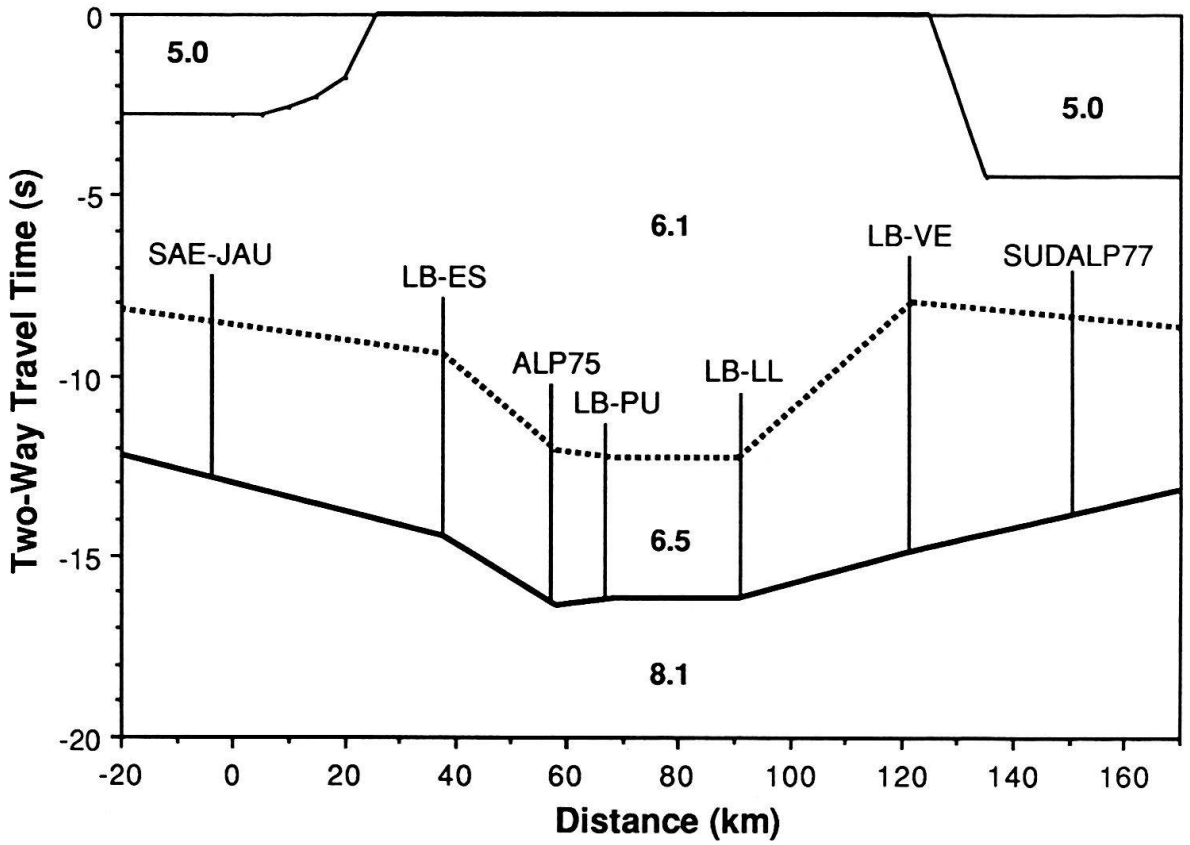

Fig. 9. Unmigrated migration velocity model in two-way travel time along the EGT, derived from the velocity-depth functions of the seismic wide-angle profiles at their intersection points with the EGT. Numbers are migration velocities in km/s. Thin solid line: base of sediments; heavy dotted line: "Conrad"; heavy solid line: Moho. Zero distance corresponds to the northernmost Vibroseis-CMP of the NFP20 eastern traverse projected onto EGT (Swiss coordinates: x = 743830, y = 231530). Vertical lines mark the locations of the seismic wide-angle profiles. For location see Figure 7.

1989; YAN & MECHIE 1989) or future detailed velocity model of the crustal structure. Its only purpose and justification is to provide a large scale velocity model that allows accurate migration over the entire length of the combined NFP20 eastern and southern traverses. Due to the big spacing between the individual profiles with respect to the complexity of the surface geology and the inherently low resolution of the seismic wide-angle method at shallow levels, the velocity structure of the upper crust is probably an oversimplified average even for the purpose of migration. On the other hand migration displacements (Fig. 2) and migration errors resulting from uncertainties in velocity (Fig. 3) only become significant at middle and lower crustal levels where we are confident that the derived model accurately portrays the average velocity structure.

Since the interfaces of the velocity model are not horizontal, the reflection points are not located vertically beneath the refraction profiles and consequently have to be migrated as well, before serving as input for the migration of the digitized line drawings. This was achieved by converting the velocity contours into two-way travel time (Fig. 9) and then migrating them in the same way as the reflection data. The likely uncertainties in travel-time correlation and subsequent interpretation of the seismic wide-angle data led to an uncertainty in the average crustal velocity around 0.2 km/s. This results in a horizontal and vertical mispositioning of the migrated velocity structure of the order of 2 km at Moho depth (Fig. 3). Since this error is fed back linearly into the migration of the line drawings the resulting error is of the same order.

Profile Combination and Depth Migration

Unlike the ECORS Pyrenees line (ECORS PYRENEES TEAM 1988; CHOUKROUNE & ECORS TEAM 1989) and the ECORS-CROP line across the western Alps (BAYER et al. 1987; NICOLAS et al. 1990) the NFP20 Alpine traverses had to be acquired in the form of several individual lines (cf. FREI et al. 1989; VALASEK et al. 1990, 1991). For the purpose of a unifying seismic study this is unfortunate, since it requires the combination of the individual profiles in order to gain an acoustic image across the central Alpine arc along the EGT. With the strong lateral variations of surface geology in the Penninic domain any such combination of laterally offset seismic reflection profiles is bound to be a subjective and in certain aspects insufficient compromise for the upper crust. The approach taken in this work aimed at consistency of complementary geophysical data on a crustal scale. Hence projecting horizontally along the relatively smooth east-west trend of the «Ivrea-corrected» Bouguer gravity isolines (KISSLING 1980, 1984; KISSLING et al. 1983) is considered to be sensible for the middle and lower crust as well as the Insubric Line, which follows the trend of the gravity field and – unlike most other Penninic structures (PFIFFNER et al. 1990b) – does not have an eastward axial plunge. The gravity effect of the Ivrea Body must be subtracted from the original Bouguer gravity anomalies because it is not considered to be present in the subsurface imaged by NFP20 eastern and southern traverses (KISSLING 1980, 1984; SCHWENDENER 1984; SCHWENDENER & MUELLER 1990).

Since upper crustal effects are not represented in this trend of the corrected Bouguer gravity anomalies this approach leads to inconsistencies in the upper crustal reflectivity patterns and their geological interpretation: although it is not entirely clear

how to correlate the Penninic gneiss nappes of the Ticino with those of the Grisons (Fig. 7), the base of the upper crustal reflectivity on line S1 at 2 to 3 s travel time does not correspond to the base of the Tambo nappe on line ET (cf. PFIFFNER et al. 1990a) as suggested by this projection technique. Geologic contour maps of the Penninic zone (PFIFFNER et al. 1990b) infer that potential upper crustal reflectors in this area are "bumpy" surfaces with considerable – but not uniform – eastward axial plunge. We cannot think of any migration and combination method of sub-parallel profiles that would accurately restore the geometric distortions introduced by the two-dimensional seismic imaging of such three-dimensional structures except by means of densely spaced cross-lines.

Figure 10 shows the unmigrated composite time section resulting from the projection of the NFP20 eastern (Fig. 8a) and southern (Fig. 8b, c, d) traverses along the east-west running trend of the "Ivrea-corrected" Bouguer gravity anomalies (KISSLING 1984) onto the EGT (Fig. 7). Though this profile already shows some aspects of the integrated fine structure of the crust below the central Alps, it still represents a severely distorted acoustic image (as e.g. illustrated by the numerous conflicting reflector dips) because migration and depth conversion have not yet been performed. Figure 11 shows the image resulting from the ray theoretical depth migration of the time section shown in Figure 10 using the velocity structure sketched in Figure 9. The most crucial test for any projection and migration method is the correlation between the resulting acoustic image and known or interpretable parts of the geological structure of the subsurface. In the case of the NFP20 eastern and southern traverses the mylonite zone of the Insubric Line is the only well documented geologic feature that is believed to be unambiguously imaged by the seismic data. As can be seen on Figure 11 the migrated reflections from the Insubric Line neatly project into its mapped outcrop location.

Moreover, a correctly performed projection and migration procedure does result in a spatial deconvolution of the dataset, i.e., it increases its spatial resolution by removing the effects of geometric spreading and reducing "cross dip" effects (BERKHOUT & VAN WULFFTEN PALTHE 1979). Ray theory assumes that the input data have perfect resolution and therefore does not remove the effects of geometric spreading. However, the amount of conflicting dips has been reduced and the "crispness" and thus the interpretability of the migrated section has been increased (compare Figs. 10 and 11). On the other hand the new cross dips appearing particularly in the upper part of the migrated section point to effects from the third dimension and/or insufficiencies of the used projection method and migration velocity model. Finally, the simultaneous depth migration of the seismic reflection and refraction data leads to an amazingly good agreement between the refraction Moho and the base of the reflective lower crust, i.e., the "reflection Moho" (cf. KLEMPERER et al. 1986; BRAILE & CHIANG 1986), which is a most important criterion for the correctness of the used migration and projection technique on a crustal scale. On the other hand the generally good agreement between the "Conrad" discontinuity (cf. LITAK & BROWN 1989) interpreted from the seismic refraction data and the top of the reflective lower crust (cf. MOONEY & BROCHER 1987; WEVER 1989) suggested by Figure 11 should not be over-emphasized, because overall both features are poorly defined.

Although the points made above by no means represent a formal proof of the correctness of the projection and the migration approach taken in this work, they never-

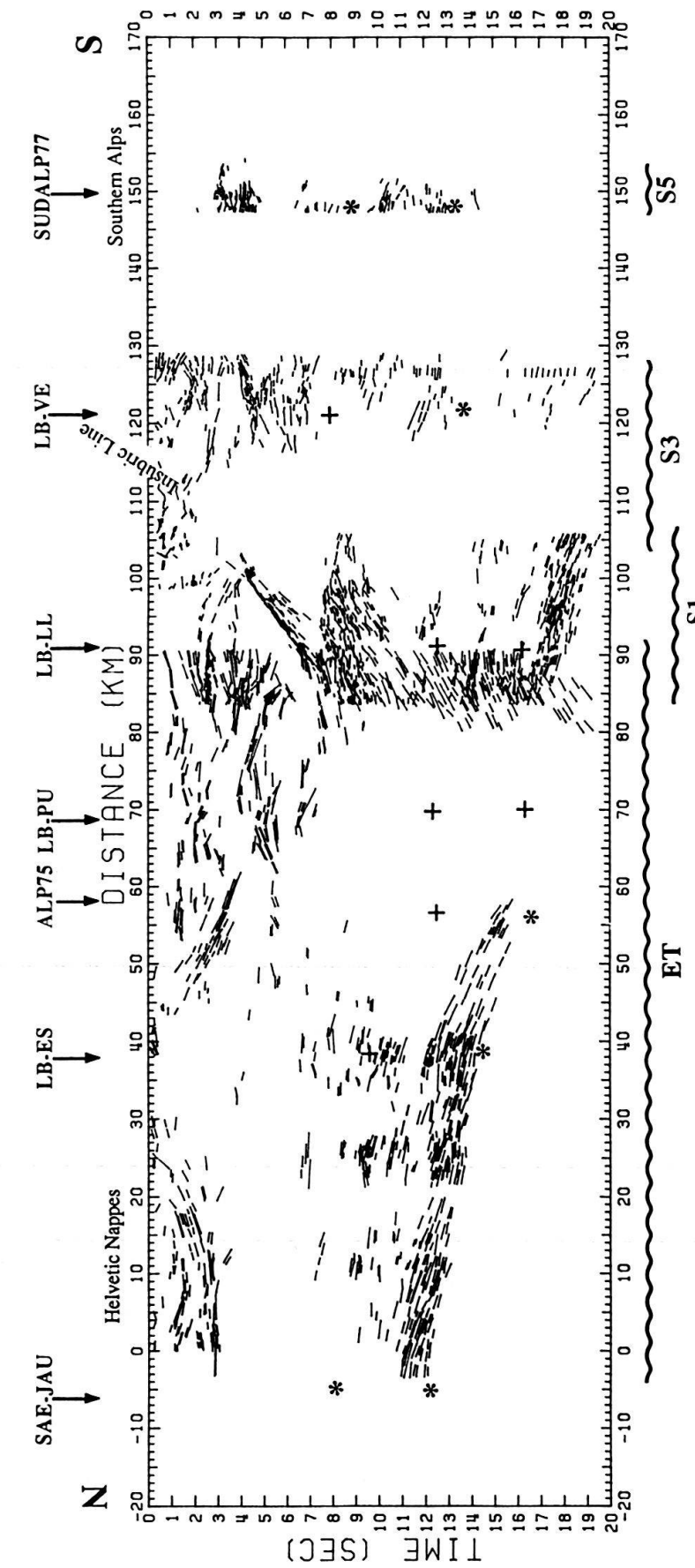

Fig. 10. Unmigrated time section resulting from the projection of the NFP20 eastern and southern traverses onto the EGT along the east-west trend of the "Ivrea corrected" Bouguer gravity anomalies (Kissling 1984). Zero distance as in previous figure. EGT shot D (Säntis) corresponds to the location of the Säntis-Jaunpass profile (SAE-JAU). The intersection of the EGT with the Insubric Line and its dip at the surface are indicated by the corresponding label. Clear, unambiguous wide-angle reflections are represented by stars, less clear ones by crosses. Horizontal and vertical scales are 1:1 for an average crustal velocity of 6.0 km/s. For location see Figure 7.

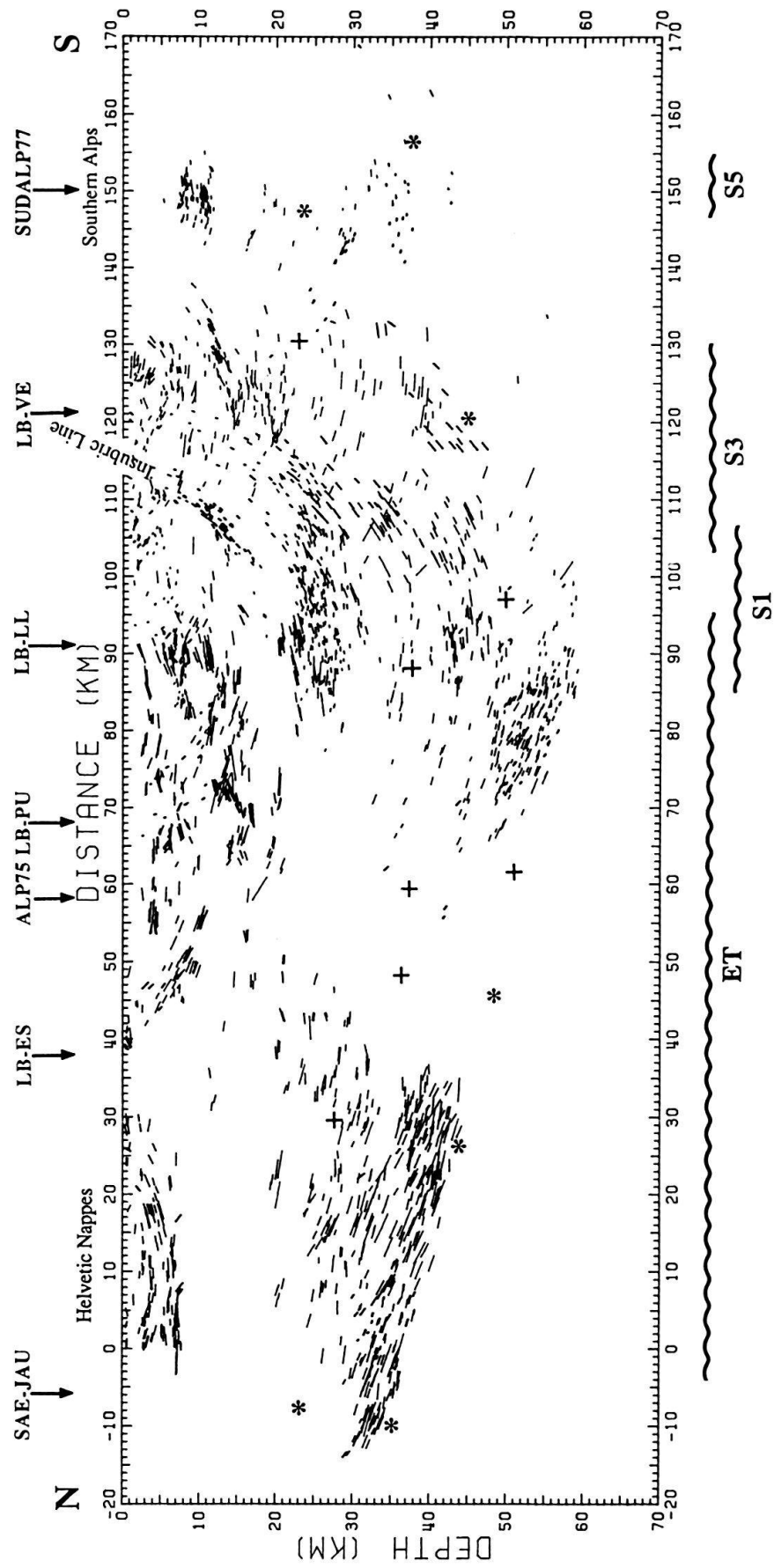

Fig. 11. Depth migration of Figure 10. Velocities used for migration: sediments 5.0 km/s (Molasse Basin and Southern Alps), upper crust, 6.1 km/s, lower crust 6.5 km/s, upper mantle 8.1 km/s (Figure 9). Clear, unambiguous wide-angle reflections are represented by stars, doubtful ones by crosses. Please note that the interfaces of the velocity model (depicted by stars and crosses for the "Conrad" and the Moho) have been migrated as well. Horizontal and vertical scales are 1:1. For location see Figure 7.

theless significantly increase the confidence one may have in the resulting depth migrated acoustic image of the Alpine crust shown in Figure 11.

Interpretation

At the northern end of the depth migrated profile shown in Figure 11 there is good agreement between the refraction and the reflection Moho (cf. KLEMPERER et al. 1986; BRAILE & CHIANG 1986). After migration they both dip south at an angle of approximately 15 degrees. From the fact that the basement north of the Aar Massif has seen no or only little internal deformation during the Alpine orogeny (PFIFFNER et al. 1990a) we may conclude that the origin of the reflections from the European Moho and probably also of the sporadic "Conrad" reflectors are of pre-Alpine age. With the onset of the upper crustal Penninic reflectivity (at a distance around 40 to 50 km) the lower crust and the Moho abruptly cease to be reflective. The strong, multicyclic and laterally discontinuous Penninic reflectivity reaches down to a depth of 15 to 20 km. It is considered to arise from a "subhorizontal" stack of crystalline nappes separated by thin slivers of sediments (PFIFFNER et al. 1990a).

Just north of the Insubric Line at a distance of 70 to 90 km from the northern end of line ET and in a depth between 50 to 60 km (Fig. 11) there is a deep reflection package whose overall character and dip lines up with those of the European reflection Moho lost some 30 km further north and east. If this feature in fact represents the southern continuation of the European reflection Moho lost in the area of strong upper crustal reflectivity in the Penninic domain, then our acoustic image clearly depicts the subduction of at least 10 km of the lowermost European crust below the Adriatic promontory of the African plate at a low angle (15 to 20 degrees). As evident from Figure 11 this interpretation is compatible with the migrated Moho points inferred from the seismic wide-angle data. In fact an amazingly similar topography of the Moho and the lower crust emerges from seismic reflection and refraction data in the western Alps (BAYER et al. 1987; ECORS-CROP DEEP SEISMIC SOUNDING GROUP 1989) and in the Pyrenees (ECORS PYRENEES TEAM 1988; CHOUKROUNE & ECORS TEAM 1989; DAIGNIERES et al. 1982). Similar to the southward downdip of the European Moho and lower crust beneath the Molasse basin and in agreement with the strongly asymmetric Alpine "Moho trough" interpreted by MUELLER et al. (1976, 1980), Figure 11 supports a northward downbending the Adriatic Moho and lower crust.

Therefore, assuming a pre-Alpine age for the origin of the reflections from the Moho and the lower crust and an alpine age for the origin of the reflections from the upper crust, the following large scale tectonic model is quite naturally advocated by the combined depth migrated NFP20 eastern and southern traverses shown in Figure 11:

With the onset of continental collision in late Eocene times subduction of European lower crust continued – possibly due to a self-sustaining driving mechanism such as the one suggested by FLEITOUT & FROIDEVAUX (1982) – though at rather low rate (<0.5 cm/y for an estimated neoalpine shortening of 100 to 200 km [TRÜMPY 1980; PFIFFNER 1986; COWARD & DIETRICH 1989]). The fact that the crustal thickness of the European and Adriatic continental margins had been previously dramatically reduced as a result of Triassic and Jurassic rifting may have facilitated early crustal shortening

and subduction. The meeting of the two "mature" crusts in the Oligocene (cf. TRÜMPY 1980) led to a space problem which in turn resulted in a downbending of the Adriatic Moho and lower crust, wedging at mid-crustal levels (MUELLER et al. 1980; KAHLE et al. 1980), backthrusting and vertical movements at upper crustal levels (HEITZMANN 1987; PFIFFNER et al. 1990a) as well as in the uplift of the external massifs and the progression of nappe formation and subhorizontal thrusting into the Alpine forelands (TRÜMPY 1980; COWARD & DIETRICH 1989). The downbending of the Adriatic Moho and lower crust suggested by MUELLER et al. (1976, 1980) and by Figure 11 can in fact account for most of the interpreted late neoalpine shortening of the upper crust in the Southern Alps (LAUBSCHER 1985, 1989; ROEDER 1989). However, the simultaneous near vertical subduction or "Verschluckung" of both the European and the African lithospheres as postulated by LAUBSCHER (1970, 1971) cannot be substantiated on the basis of the available seismic reflection data. Wedging at mid-crustal levels has been previously inferred by KAHLE et al. (1980) and KISSLING (1980, 1982) from the presence of a distinct local gravity high in the Ticino, and by MUELLER et al. (1980), based on the detailed interpretation of seismic wide-angle data and by PFIFFNER et al. (1990a) and PFIFFNER (1990) from the seismic reflection data. In the low-pass filtered reinterpretation of some of these profiles used for the purpose of this work the thickening of the slow upper crust relative to the fast lower crust (see Figs. 9, 10 and 11) in the axial zone of the Alps may be considered as an indication of mid-crustal wedging in conjunction with lower crustal subduction. Vertical movements of upper crustal rocks in the contact zone of the European and Adriatic plates occurred along the highly reflective mylonite zone of the Insubric Line (SCHMID et al. 1987, 1989; FOUNTAIN et al. 1984). The fact that after migration the reflections from the Insubric Line are confined to the upper crust (Fig. 11) may be taken as further indirect evidence for subhorizontal wedging in the middle crust. The topography of the refraction and reflection Mohos suggests that at least the recent parts of the neoalpine subduction of the European lower crust and upper mantle have occurred at a low angle of 15 to 20 degrees (Fig. 11). Since the lower crust seems to have been decoupled with the tectonic from the upper crust and since the original positions of the observed Moho reflections are unknown, the total amount of this low angle subduction can hardly be quantified. The tectonic interpretation of Figure 11 is schematically illustrated in Figure 12.

The above tectonic model represents one possible explanation of the reflectivity distribution within the Alpine crust shown in Figure 11. One has to bear in mind that this image is nothing but an acoustic snapshot of the present-day physical state of the crust below the central Alps, in which certain important tectonic features may have found no expression at all, whereas some other rather unimportant aspects may well be overemphasized. However, with all its crudeness and limitations, we consider the above explanation to be an attractive and appealing one, because it is in good qualitative agreement with the relatively well established post-Eocene tectonic evolution of the Alps and the mass balance considerations derived therefrom as well as with the most pertinent complementary geophysical information, such as the pronounced asymmetry of the Moho "trough", the low average crustal velocity in the Penninic domain (MUELLER et al. 1980), the local gravity high in the Ticino (KAHLE et al. 1980; KISSLING 1980) and the presence of a lithospheric root required by gravity (KISSLING 1982; KISSLING et al. 1983; SCHWENDENER 1984; SCHWENDENER & MUELLER 1990),

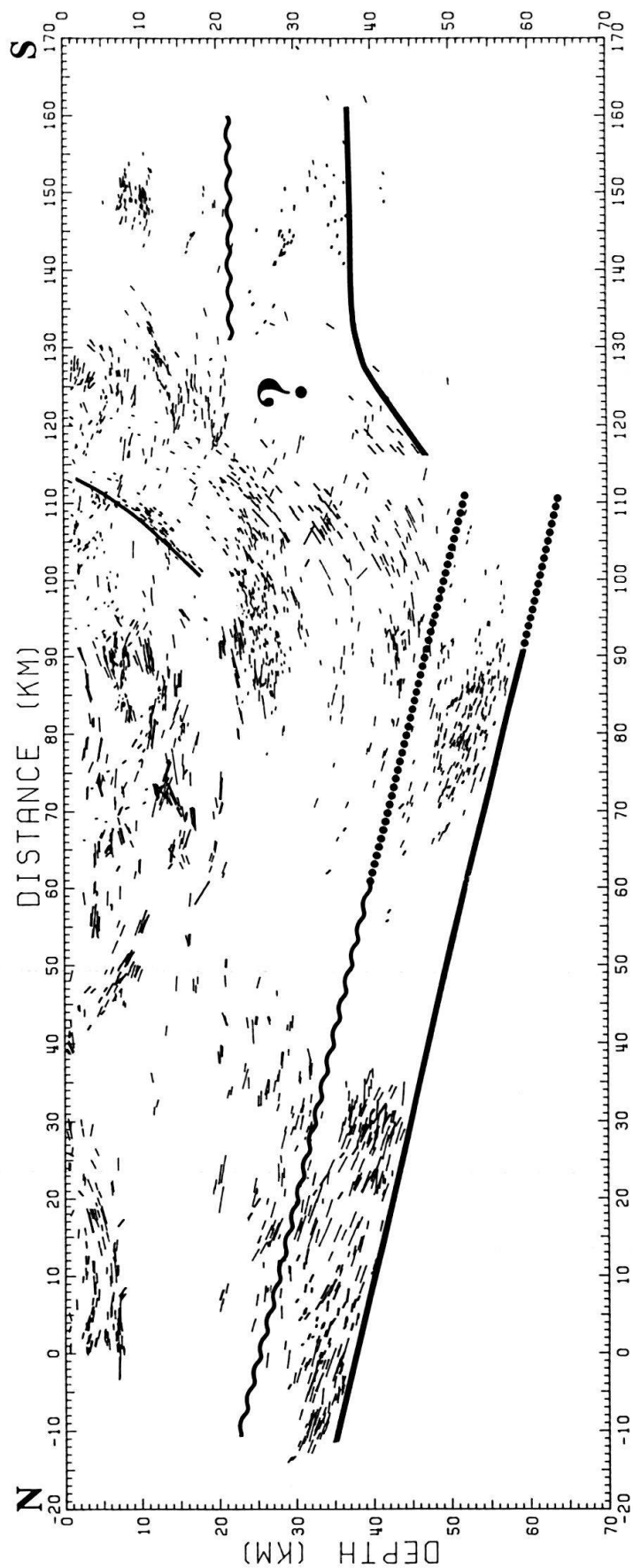

Fig. 12. Large-scale tectonic interpretation of Figure 11. Heavy line: course of the Moho as documented by the migrated seismic wide-angle and normal-incidence reflections; wavy line: top of the lower crust as inferred from the seismic wide-angle data; dotted line: interpreted continuation of the European Moho and lower crust; thin solid line: reflection segments from the Insubric Line. The question mark refers to the unknown continuation of the Adriatic middle and lower crust into the European crust and thus to the speculative nature of middle crustal tectonics and orogenic crustal thickening on the basis of the presently available data. Horizontal and vertical scales are 1:1. For location see Figure 7.

surface wave dispersion analysis (PANZA et al. 1980) and teleseismic delay times (BAER 1979, 1980).

The geometric inconsistency between the gently south dipping subduction of the European lower crust and uppermost mantle shown in Figures 11 and 12 and the near-vertical orientation of the lithospheric root inferred from the analysis of surface wave dispersion (PANZA et al. 1980) and teleseismic delay times (BAER 1979, 1980) can be explained as follows: first, the acoustic image derived in the course of this work (Figs. 11 and 12) reaches to a depth of only some 60 km; second, the mentioned geophysical methods (surface wave dispersion, early versions of teleseismic delay time studies) used to interpret the near-vertical orientation of the lithospheric slab at greater depth have a low resolution even on a lithospheric scale. In addition, post-Eocene Alpine tectonics can be as readily explained by the south and east dipping subduction of the European plate (cf. PFIFFNER et al. 1990a and BUTLER 1986) as with the simultaneous near-vertical subduction of both the European and the Adriatic plates (cf. LAUBSCHER 1970, 1971). First results from modern teleseismic tomography favour a non-vertical orientation of the subducted lithospheric slab at greater depth (SPAKMAN 1990).

The simultaneous migration of the interfaces interpreted from the seismic refraction data and the line drawings of the seismic reflection data has removed seemingly inconsistencies (e.g. PFIFFNER et al. 1988) between the refraction and the reflection Moho in that there is no solid evidence upon which to postulate a continuous refraction Moho across the Alpine arc. Both the reflection and the refraction Mohos, where defined, now nicely depict a gently (10 to 20 degrees) south-dipping subduction of the upper mantle and parts of the lower crust of the European plate beneath the Adriatic promontory of the African plate (HOLLIGER 1990, 1991). There are two different aspects to the discontinuity of the reflection Moho: first, the rather abrupt loss of the reflection Moho south of the Aar Massif in the Penninic domain (approximately from 35 to 65 km distance on migrated data shown in Figures 11 and 12); second, the reappearance of the reflection Moho just south of the Insubric Line at a substantially greater depth than the one inferred for the Adriatic refraction Moho from seismic wide-angle data (cf. Figs. 10, 11 and 12). This in turn suggests that the discontinuity of the reflection Moho below the Penninic nappes of the Grisons (Fig. 7) most likely represents a seismic imaging problem. Reflections from the Moho and the lower crust are also lacking in the axial parts of the western Alps (NICOLAS et al. 1990) profile and are strongly "washed out" on the Pyrenees (CHOUKROUNE & ECORS TEAM 1989) profile. From all these "transparent" areas clear wide-angle reflections from the Moho have been reported (cf. Figs. 10 and 11; the ECORS-CROP DEEP SEISMIC SOUNDING GROUP 1989; DAIGNIERES et al. 1982).

In the case of NFP20 data the lack of normal-incidence reflections from the Moho where there are wide-angle reflections may be attributed to either insufficient source energy to penetrate the deep parts of the thickened orogenic crust, defocusing of the reflected energy out of the used receiver spread by the geometry of the reflector (VALASEK et al. 1990) or destruction of the Moho reflectors by intense deformation (PFIFFNER et al. 1990a). The energy argument seems unlikely because similar or weaker charges have imaged the Moho at substantially greater depth further to the south. Furthermore, the excellent imaging of the upper 5 to 10 s travel time (cf.

PFIFFNER 1990) indicates that the S/N is not worse than elsewhere along the traverse. Defocusing effects seem unlikely because the slope of the Moho constrained by seismic wide-angle reflections (Figs. 11 and 12) does not change in the Penninic domain. In the light of the above arguments interpreting the non-reflective lower crustal region as the deformed contact zone due to wedging of the European and Adriatic crusts (PFIFFNER 1990) cannot be discarded. We interprete the discontinuity of the lower crustal reflectivity and the discrepancy between the reflection and the refraction Moho beneath the Penninic zone as a seismic imaging problem. It is noteworthy that the loss of the Moho reflections coincides with the strongest upper crustal reflectivity in the Penninic domain and the reappearance of the Moho reflections with the weakening of the Penninic reflectivity (Figs. 10 and 11). CARBONELL & SMITHSON (1990) have shown by finite difference modelling of the full wave field that the imaging of highly reflective zones may not be possible if the wave front is broken up by "rough" reflectors (such as the potential reflectors in the Penninic zone [PFIFFNER et al. 1990b]) in the overburden. Such scattering phenomena represent source-generated noise and hence for the same frequency spectrum become more severe with increasing source strength. If a broken up wave front is "reflected" from an interface, the recorded seismic section shows no lateral coherence in terms of phases but only in terms of wave groups, i.e., energy accumulations. Therefore the presence of the reflecting interface is only detectable on spatially aliased seismic wide-angle data but not on normal-incidence seismic reflection data. Scattering due to the complex upper crustal geology in the Penninic domain of the Alps and the axial zone of the Pyrenees therefore represents a plausible qualitative explanation for the apparent discontinuity of the underlying reflection Moho.

Discussion

In the methodological part of this work we have shown how important the migration of deep seismic reflection data is and how sensitive this process is to an accurate parametrisation of the velocity field. We argue that in the case of deep seismic reflection data ray theoretical migration of the observed travel times, i.e., of a digitized line drawing of the observed primary reflections and diffractions, represents *the* viable alternative to migrating the "full" observed wave field using algorithms based on the scalar wave equation. Ray theory represents a crude first order approximation of the wave equation for high frequencies and for this reason does not suffer from the data insufficiencies hampering wave equation migration. Ray theoretical migration is geometrically accurate and numerically efficient, can handle very complex velocity structures and is able to account for geometric focusing and defocusing effects; as a high frequency approximation it does, however, assume perfect resolution of the stacked input data and therefore, unlike wave equation migration, does not increase the spatial resolution of the migrated section by collapsing the Fresnel zone. The migration method discussed in this paper is able to correct for simple effects from the third dimension such as an oblique orientation of the profile with respect to the tectonic grain and a uniform axial plunge of the imaged geologic structures [see formulae (7) and (8)]. The geometric restoration of complicated three-dimensional effects such

as the reflections arising from the "bumpy" interfaces of the Penninic nappe system (PFIFFNER et al. 1990b) are, however, clearly beyond the potential of any migration method at present.

We think that the major objection against ray theoretical migration, which concerns the inherent subjectivity of the hand-made line drawings and their lack of amplitude and phase information, is largely invalidated by the fact that – as mentioned above – computer generated line drawings used to trick conventional algorithms (cf. VALASEK et al. 1990; MILKEREIT 1987) are subjective as well and are unlikely to contain much original amplitude and phase information. Finally one must not forget that until the early 1970s virtually all the oil discoveries – amongst them some of the worlds biggest hydrocarbon reserves – were made based on ray migration of "picked" time sections and that ray theoretical depth migration of interpreted time horizons is still standardly used by the oil industry (SATTLEGGER 1982).

Deep seismic reflection profiles represent acoustic snapshots of the present physical state of the middle and lower crust, which almost everywhere is the result of a complicated, multiphase tectonic history. Moreover, every tectonic event can have different impacts at different crustal levels (e.g. FURLONG & FOUNTAIN 1986; MCKENZIE & BICKLE 1988), simultaneously create new reflectivity patterns and destroy older ones or find no expression at all in the crustal reflectivity. Therefore in addition to the uncertainties on the physical origin of deep seismic reflections (e.g. MATTHEWS 1986; WARNER 1990a) there often is a considerable uncertainty on the age of their formation (cf. KLEMPERER et al. 1990). As a consequence the tectonic interpretation of deep seismic reflection data is – even after proper processing and migration – anything but straightforward and every effort must be made to substantiate it by using complementary geological and geophysical information. The central Swiss Alps are one of the few regions where – despite formidable tectonic complications – a correlation of seismic reflection patterns and associated geologic structures is possible at upper crustal levels (PFIFFNER et al. 1988, 1990a). At greater depth, however, this direct approach is no longer feasible and the interpretation has to rely on a combination of the results of geophysical methods and complementary tectonic ideas extrapolated from surface geology. Whereas the experienced geologist may be able to confirm or discard certain tectonic principles by qualitative arguments on the basis of the unmigrated seismic data depth migration and profile combination are a *conditio sine qua non* for the comparison of the reflectivity distribution with other geophysical parameters. Moreover, the huge migration displacements at middle and lower crustal levels (Fig. 2) give rise to a substantial speculative component in tectonic interpretations derived from the unmigrated data.

We have interpreted the reflectivity distribution resulting from the ray theoretical depth migration of the combined NFP20 eastern and southern traverses (Figs. 11 and 12) as being the acoustic expression of nappe emplacement and vertical escape movements in the upper crust, wedging at middle crustal levels, and subduction of the European lower crust. Though discrepancies may exist in detail this model is compatible with today's ideas of large scale neoalpine tectonics and mass balance considerations as well as with all the complementary geophysical information. In fact most of these general mechanisms have been previously suggested by other workers to explain preliminary results from unmigrated NFP20 seismic reflection profiles (PFIFFNER et al.

1988, 1990a; PFIFFNER 1990; FREI et al. 1989; VALASEK et al. 1991). We do consider it as the merit of this work to provide a combination and simultaneous depth migration of the deep seismic reflection profiles of the NFP20 eastern and southern traverses and the complementary seismic wide-angle data. The resulting acoustic images (Figs. 11 and 12) are believed to be consistent at middle and lower crustal levels where migration displacement – and hence interpretational uncertainties – are substantial and thus allow to quantitatively constrain or relativate some arguments of previous qualitative studies concerning the deeper crustal levels of the Alpine edifice. Figures 11 and 12 put clear constraints on the shallow geometry of the central Alpine subduction zone, the amount of recent crustal subduction and the geometry and depth extent of the Insubric Line. However, the tectonics of the middle crust, which can only be inferred indirectly, and the geometry of the subduction zone at greater depth remain speculative (Fig. 12). We are therefore of the opinion that thoroughly planned and coordinated future research concentrating on the geometry of the Alpine subduction zone as well as on the mechanisms of crustal shortening and subduction will be scientifically highly rewarding. A potential sequence of geophysically oriented research topics might involve: local tomographic studies – possibly involving active sources – to derive detailed images from the middle and upper crust (cf. KISSLING 1988; KRADOLFER 1989), detailed teleseismic tomography (cf. DZIEWONSKI & ANDERSON 1984; SPAKMAN 1990) to constrain the geometry of the subducted lithosphere at depths not accessed by this study, i.e., below 60 km, and a reevaluation of the gravity database (KISSLING 1980, 1982; SCHWENDENER 1984; SCHWENDENER & MUELLER 1990) to evaluate how much lower crustal material of what density has been subducted.

Appendix

Figure 13 shows the algorithmic details of the ray theoretical depth migration process of a digitized line element defined by N points. Ray tracing is performed by numerically integrating the two-dimensional ray equation system (3) using a fifth order Runge-Kutta method with adaptive stepsize and error control (PRESS et al. 1986). Following ZELT & ELLIS (1988) the computational efficiency of the integration is enhanced by varying the integration stepsize t_{step} according to the complexity of the velocity model

$$t_{step} = \frac{\sigma}{|v_x| + |v_z|} \tag{9}$$

where $\sigma = 0.15 \pm 0.1$ is an empirically determined dimensionless constant, and v_x and v_z represent the spatial derivatives of the velocity field. The maximum stepsize must not exceed the minimum one-way travel time through the thinnest layer of the model. The desired accuracy for a single Runge-Kutta step can be estimated as follows: the allowed error resulting from the maximum expected number of integration steps must not exceed the average digitizing error involved in line drawing preparation. If the initial stepsize t_{step} determined by (9) leads to an error, which is too large, the corresponding integration step will be repeated with successively smaller stepsizes until the desired precision is obtained.

Detailed velocity information on a crustal scale is provided by seismic wide-angle data which are interpreted with only a limited number of forward ray tracing programs. It is therefore sensible to choose a parametrisation scheme which is compatible with that of the most popular forward programs such as the widely used SEIS83 (CERVENY & PSENCIK 1984) and its successors or RAY84 (LUETGERT 1988) and RAY87 (SIERRO 1988; LUETGERT 1988), which are currently used at the USGS and ETH Zürich. Such a model is displayed in Fig. 14 and can be characterized as follows: n layers are defined by n + 1 interfaces. Each interface must be continuous between the left and right margin of the model and must not intersect any other interface. Velocities are specified at the intersection points of vertical velocity lines and these interfaces. The program thus divides the model into a two-dimensional

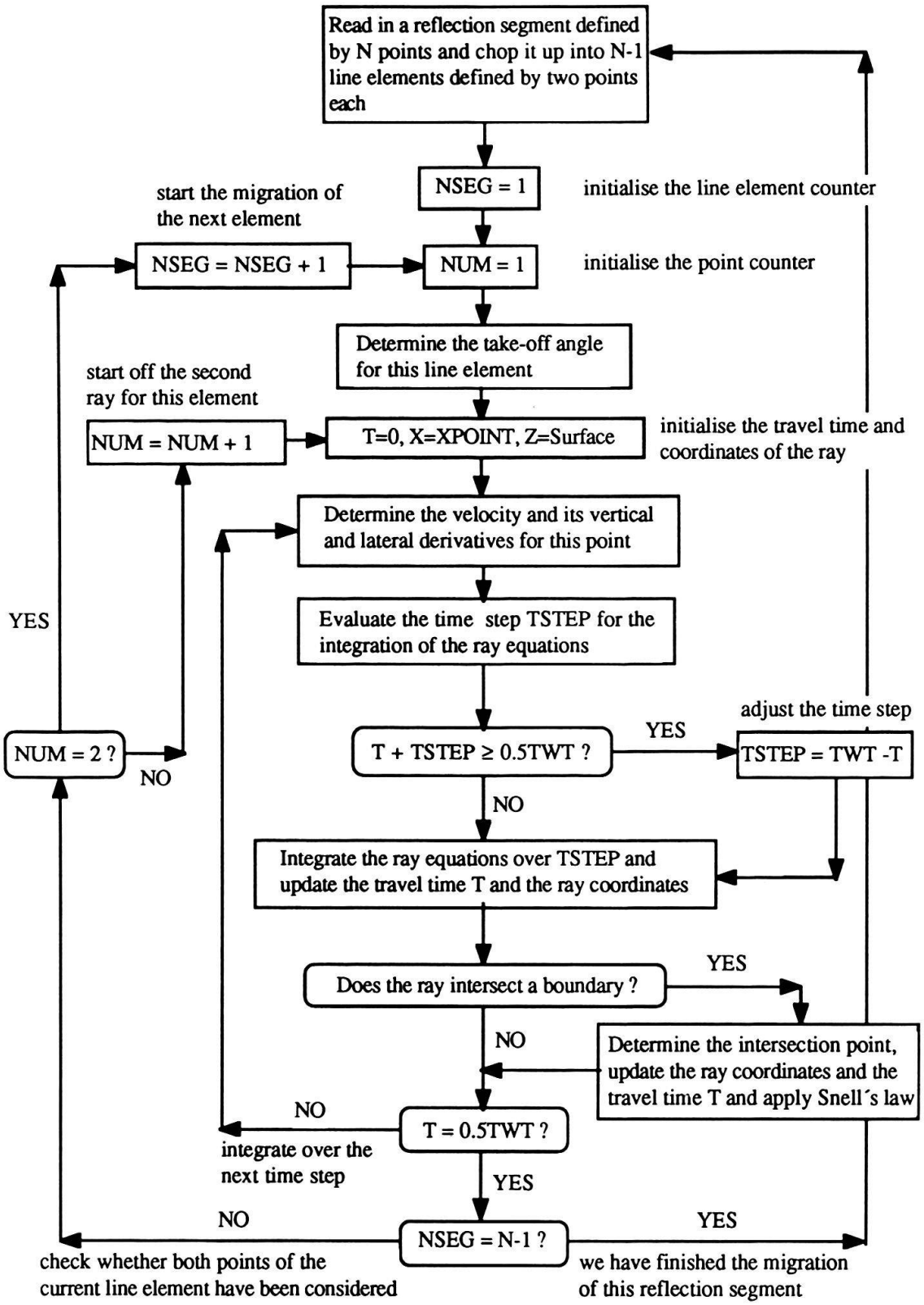

Fig. 13. Flow chart showing the algorithmic details of the ray theoretical depth migration of a digitized reflection segment defined by N points.

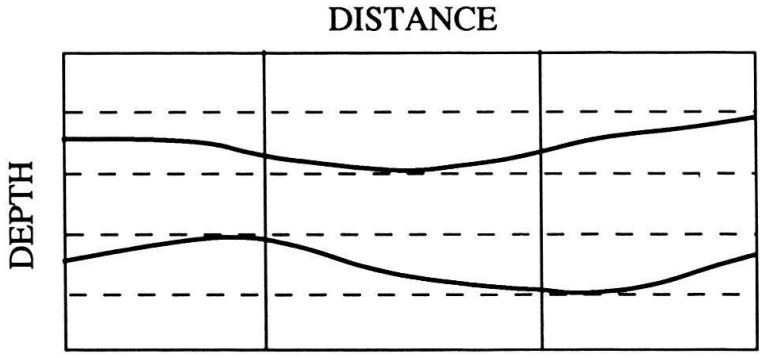

Fig. 14. Schematic illustration of the parametrisation of the velocity model for RAY84 (Luetgert 1988), RAY87 (Sierro 1988) and Migart (Holliger 1991). The user supplies the geometry of the interfaces (heavy lines), the location of the vertical velocity lines (solid vertical lines) and the velocities at the intersections of the vertical velocity lines with the interfaces; the program then generates a two-dimensional velocity grid. For an arbitrary point, its layer and grid number are evaluated, which then allows the velocity and its spatial derivatives to be determined by interpolation.

velocity grid. For converging interfaces a certain minimum vertical separation between the horizontal velocity lines will be maintained.

To solve the ray equation system (3), the velocity and its gradients must be known along the entire ray path. For the velocity model outlined above, this can be done as follows: First, find out in which layer and in which rectangle the particular ray point is, then, knowing the velocities at the corners and the gradients along the edges of the rectangle, determine the velocity and its gradients at any point within this rectangle by two-dimensional linear interpolation (cf. Press et al. 1986).

Acknowledgments

The work presented in this paper is part of a PhD thesis which was enthusiastically initiated and assisted by Stephan Mueller. The seismic reflection data considered in this work were acquired as part of the Swiss National Research Program 20 (NFP20) "Geologische Tiefenstruktur der Schweiz". We have profitted from the ready availability of these data and from the well-equipped in-house seismic processing facilities installed by NFP20 at ETH Zürich. Discussions with Jörg Ansorge, Nicolas Deichmann, Simon Klemperer, Paul Valasek and Mike Warner were inspiring and helpful. Adrian Pfiffner's and David B. Snyder's careful and efficient review helped to improve the quality of this manuscript. After already having been a visitor in winter 1986/1987 a generous fellowship of the British Natural Environmental Research Council (NERC) allowed one of us (K.H.) to spend another four wonderful and productive months at the British Institutions' Reflection Profiling Syndicate (BIRPS) in Cambridge, U.K., in summer 1988. In this context we also thankfully acknowledge the receipt of the BIRPS version of a ray migration program originally developed by Bernard Raynaud.

REFERENCES

Ansorge, J. 1989: Aspects of acquisition and interpretation of deep seismic sounding data. In: Digital Seismology and Fine Modeling of the Lithosphere, Ettore Majorana International Science Series (Physical Sciences) 42, 211–227 (Ed. by Cassinis, R., Nolet, G. & Panza, G.F.), Plenum Press, New York.

Ansorge, J., Prodehl, C. & Bamford, D. 1982: Comparative interpretation of explosion seismic data. J. Geophys. 51, 69–84.

Baer, M. 1979: Kalibrierung des neuen Stationsnetzes des Schweizerischen Erdbebendienstes im Hinblick auf die Verbesserung der Lokalisierung seismischer Ereignisse mit Epizentralentfernungen bis 100 Grad. PhD Thesis, ETH Zürich.

— 1980: Relative travel time residuals for teleseismic events at the new Swiss seismic station network. Ann. de Géophys. 36, 119–126.

Bayer, R. et al. (20 coauthors), 1987: Premiers résultats de la traversée des Alpes occidentales par sismique reflexion verticale (Programme ECORS-CROP). C.R. Acad. Sci. Paris 305 II, 1461–1470.

Berkhout, A.J. & Van Wulfften Palthe, D.W. 1979: Migration in terms of spatial deconvolution. Geophys. Prospect. 27, 261–291.

Braile, L.W. & Chiang, C.S. 1986: The continental Mohorovicic discontinuity: results from near-vertical and wide-angle seismic reflection studies. In: Reflection Seismology: A Global Perspective (Ed. by Baranzangi, M. & Brown, L.), Amer. Geophys. Union, Geodynamics Series 13, 209–222.

Brown, L.D. 1986: Aspects of COCORP deep seismic reflection profiling. In: Reflection Seismology: A Global Perspective (Ed. by Baranzangi, M. & Brown, L.), Amer. Geophys. Union, Geodynamics Series 13, 257–272.

Carbonell, R. & Smithson, S.B. 1990: The fine structure of the Moho in the Basin and Range from PmP and SmS phases of the 1986 Nevada PASSCAL reflection experiment. Terra Abstracts 2, 30.

Cerveny, V. & Psencik, I. 1984: SEIS83, In: Documentation of Earthquake Algorithms (Ed. by Engdahl, E.R.), World Data Center A for Solid Earth Geophysics, Boulder 36–40.

Choukroune, P. & ECORS Team 1989: The ECORS Pyrenean deep seismic profile reflection data and the overall structure of an orogenic belt. Tectonics 8, 23–39.

Chun, J.H. & Jacewitz, C.A. 1981: Fundamentals of frequency domain migration. Geophysics 46, 717–733.

Coward, M. & Dietrich, D. 1989: Alpine tectonics – an overview. In: Alpine Tectonics (Ed. by Coward, M.P., Dietrich, D. & Park, R.G.), Geol. Soc. Lond. Spec. Publ. 45, 1–32.

Daignieres, M., Gallart, J., Banda, E. & Hirn, A. 1982: Implications of the seismic structure for the orogenic evolution of the Pyrenean range. Earth and planet. Sci. Lett. 57, 88–100.

Deichmann, N., Ansorge, J. & Mueller, St. 1986: Crustal structure of the Southern Alps beneath the intersection with the European Geotraverse. Tectonophysics 126, 57–83.

Dohr, G. & Meissner, R. 1975: Deep crustal reflections in Europe. Geophysics 40, 25–39.

Dziewonski, A.M. & Anderson, D.L. 1984: Seismic tomography of the Earth's interior. Amer. Scientist 72, 483–494.

ECORS-CROP Deep Seismic Sounding Group 1989: Mapping the Moho of the Western Alps by wide-angle reflection seismics. Tectonophysics 162, 193–202.

ECORS Pyrenees Team 1988: Deep reflection seismic survey across an entire orogenic belt, the ECORS Pyrenees profile. Nature 331, 508–511.

Egloff, R. 1979: Sprengseismische Untersuchungen der Erdkruste in der Schweiz. PhD Thesis, ETH Zürich.

Fleitout, L. & Froidevaux, C. 1982: Tectonics and topography for a lithosphere containing density anomalies. Tectonics 1, 21–56.

Fountain, D.M., Hurich, C.A. & Smithson, S.B. 1984: Seismic reflectivity of mylonite zones in the crust. Geology 12, 195–198.

Frei, W., Heitzmann, P., Lehner, P., Mueller, St., Olivier, R., Pfiffner, A., Steck, A. & Valasek, P. 1989: Geotraverses across the Swiss Alps. Nature 340, 544–548.

Furlong, K.P. & Fountain, D.M. 1986: Continental crustal underplating: thermal considerations and seismic-petrologic consequences. J. geophys. Res. 91, 8285–8294.

Gazdag, J. & Sguazzero, P. 1984: Migration of Seismic Data. Proc. Inst. Electric. Electron. Eng. (IEEE) 72, 1302–1315.

Gibbs, A.D. 1987: Linked tectonics of the northern North Sea basins. In: Sedimentary Basins and Basin-Forming Mechanisms (Ed. by Beaumont, C. & Tankard, A.J.), Mem. Can. Soc. Petrol. Geol. 12, 163–171.

Hagedoorn, J.G. 1954: A process of seismic reflection interpretation. Geophys. Prospect. 2, 85–127.

Heitzmann, P. 1987: Evidence of late Oligocene/Early Miocene backthrusting in the central Alpine "root zone". Geodinamica Acta 1, 183–192.

Holliger, K. 1990: A composite, depth migrated deep seismic reflection section along the Alpine segment of the EGT derived from the NFP20 eastern and southern traverses. In: Results from the fifth EGT study centre (Roischolzhausen): Integrative Studies (Ed. by Freeman, R., Giese, P. & Mueller, St.), European Science Foundation, Strasbourg, 245–254.

— 1991: Ray-based image reconstruction in controlled source seismology with an application to seismic reflection and refraction data across the central Swiss Alps. PhD thesis ETH Zürich.

Holliger, K. & Klemperer, S.L. 1989: A comparison of the Moho interpreted from gravity data and from deep seismic reflection data in the northern North Sea. Geophys. J. 97, 247–258.

Junger, A. 1951: Deep basement reflections in Big Horn County, Montana. Geophysics 16, 499–505.

Kahle, H.-G., Mueller, St., Klingelé, E., Egloff, R. & Kissling, E. 1980: Recent dynamics, crustal structure and gravity in the Alps. In: Earth's Rheology, Isostasy and Eustasy (Ed. by Moerner, N.A.), John Wiley and Sons, New York 377–388.

Kissling, E. 1980: Krustenaufbau und Isostasie in der Schweiz. PhD Thesis, ETH Zürich.

Kissling, E. 1982: Aufbau der Kruste und des oberen Mantels in der Schweiz, Geodätisch-Geophysikalische Arbeiten in der Schweiz. Schweizerische Geodätische Kommission 35, 37–126.

— 1984: Three-dimensional gravity model of the northern Ivrea-Verbano zone. In: Geomagnetic and Gravimetric Studies in the Ivrea Zone (Ed. by Wagner, J.-J. & Mueller, St.), Matériaux pour la Géologie de la Suisse, Géophysique 21, 53–61.

— 1988: Geotomography with local earthquake data. Rev. Geophys. 26, 659–698.

Kissling, E., Mueller, St. & Werner, D. 1983: Gravity anomalies, seismic structure and geothermal history of the Central Alps. Annales Geophysicae 1, 37–46.

Klemperer, S.L. 1989: Processing of BIRPS deep seismic reflection data: a tutorial review. In: Digital Seismology and Fine Modeling of the Lithosphere, Ettore Majorana International Science Series (Physical Sciences) 42 (Ed. by Cassinis, R., Nolet, G. & Panza, G.F.), Plenum Press, New York 229–257.

Klemperer, S.L., Hauge, T.A., Hauser, E.C., Oliver, J.E. & Potter, C.J. 1986: The Moho in the northern Basin and Range Province, Nevada, along the COCORP 40°N seismic reflection transect: Geol. Soc. Amer. Bull. 97, 603–618.

Klemperer, S.L., Hobbs, R.W. & Freeman, B. 1990: Dating the source of lower crustal reflectivity using BIRPS deep seismic profiles across the Iapetus suture. Tectonophysics 173, 445–454.

Kradolfer, U. 1989: Seismische Tomographie in der Schweiz mittels lokaler Erdbeben. PhD Thesis, ETH Zürich.

Laubscher, H.P. 1970: Bewegung und Wärme in der alpinen Orogenese. Schweiz. min. petr. Mitt. 50, 565–596.

— 1971: Large-scale kinematics of the western Alps and northern Apennines and its palinspastic implications. Amer. J. Sci. 271, 193–226.

— 1985: Large-scale, thin-skinned thrusting in the southern Alps: kinematic models. Geol. Soc. Amer. Bull. 96, 710–718.

— 1989: The tectonics of the southern Alps and the Austro-Alpine nappes: a comparison. In: Alpine Tectonics (Ed. by Coward, M.P., Dietrich, D. & Park, R.G.), Geol. Soc. Lond. Spec. Publ. 45, 229–242.

Levin, F.K. 1971: Apparent velocity from dipping interface reflections. Geophysics 36, 510–516.

Lindsey, J.P. 1989: The Fresnel zone and its interpretive significance. Geophysics: The Leading Edge of Exploration (October 1989), 33–39.

Litak, R.K. & Brown, L.D. 1989: A modern perspective on the Conrad discontinuity. EOS 70, 713 and 722–725.

Luetgert, J.H. 1988: User's Manual for RAY84/RAY83PLT interactive two-dimensional raytracing/synthetic seismogram package. USGS Open-File Report 88–238, Menlo Park.

Matthews, D.H. 1986: Seismic reflections from the lower crust around Britain. In: The Nature of Lower Continental Crust (Ed. by Dawson, J.B., Carswell, D.A., Hall, J. & Wedepohl, K.H.), Geol. Soc. Lond. Spec. Publ. 24, 11–22.

Maurer, H. 1989: Die Struktur der Erdkruste unter dem schweizerischen Alpennordrand. Diploma Thesis, ETH Zürich.

McKenzie, D. & Bickle, M.J. 1988: The volume and composition of melt generated by extension of the lithosphere. J. Petrol. 29, 625–679.

Milkereit, B. 1987: Migration of noisy crustal seismic data. J. geophys. Res. 92, 7916–7930.

Mooney, W.D. & Brocher, T.M. 1987: Coincident seismic reflection/refraction studies of the continental lithosphere. Rev. Geophys. 25, 723–742.

Mueller, St., Ansorge, J., Egloff, R. & Kissling, E. 1980: A crustal cross section along the Swiss Geotraverse from the Rhinegraben to the Po Plain. Eclogae geol. Helv. 73, 463–483.

Mueller, St. & Banda, E. 1983: The European Geotraverse project. Terra Cognita 3, 291–294.

Mueller, J., Egloff, St. & Ansorge, J. 1976: Struktur des tieferen Untergrundes entlang der Schweizer Geotraverse. Schweiz. min. petrogr. Mitt. 56, 685–692.

Nicolas, A., Hirn, A., Nicolich, R., Polino, R. & The ECORS-CROP Working Group 1990: Lithospheric wedging in the western Alps inferred from the ECORS-CROP traverse. Geology 18, 587–590.

Panza, G.F., Mueller, St. & Calcagnile, G. 1980: The gross features of the lithosphere-asthenosphere system in Europe from seismic surface and body waves. Pageoph 118, 1209–1213.

Pfiffner, A.O. 1986: Evolution of the north Alpine foreland basin in the Central Alps. Spec. Publ. Int. Assoc. Sediment. 8, 219–228.

— 1990: Crustal shortening of the Alps along the EGT profile. In: Results from the fifth EGT study centre (Roischolzhausen): Integrative Studies (Ed. by Freeman, R., Giese, P. & Mueller, St.), European Science Foundation, Strasbourg, 255–262.

Pfiffner, A.O., Frei, W., Finckh, P. & Valasek, P. 1988: Deep seismic reflection profiling in the Swiss Alps: explosion seismology results for line NFP 20-EAST. Geology 16, 987–990.

Pfiffner, A.O., Frei, W., Valasek, P., Stäuble, M., Dubois, L. & Schmid, S. 1990a: Deep seismic reflection profiling in the Swiss Alps: Vibroseis results and geologic interpretation for line NFP 20-EAST. Tectonics 9, 1327–1355.

Pfiffner, A.O., Klaper, E.M., Mayerat, A.-M. & Heitzmann, P. 1990b: Structure of the basement-cover contact in the Swiss Alps. In: Deep Structures of the Alps (Ed. by Roure, F., Heitzmann, P. & Polino, R.), Mém. Soc. géol. France 155, Mém. Soc. géol. Suisse 1, Soc. geol. Ital. Vol. spec. 1, 247–262.

Press, W.H., Flannery, B.P., Teukolsky, S.A. & Vetterling, W.T. 1986: Numerical Recipes – The Art of Scientific Computing. Cambridge University Press, Cambridge.

Raynaud, B. 1988a: Diffraction modelling of three-dimensional lower crustal reflectors. Geophys. J. 93, 149–161.

— 1988b: A 2-D, ray-based, depth migration method for deep seismic reflections. Geophys. J. 93, 163–171.

Robinson, E.A. 1983: Migration of Geophysical Data. Reidel, Dodrecht.

Roeder, D. 1989: South-Alpine thrusting and trans-Alpine convergence. In: Alpine Tectonics (Ed. by Coward, M.P., Dietrich, D. & Park, R.G.), Geol. Soc. Lond. Spec. Publ. 45, 211–228.

Sattlegger, J. 1982: Migration of seismic interfaces. Geophys. Prospect. 30, 71–85.

Schmid, S.M., Aebli, H.R., Heller, F. & Zingg, A. 1989: The role of the Periadriatic Line in the tectonic evolution of the Alps. In: Alpine Tectonics (Ed. by Coward, M.P., Dietrich, D. & Park, R.G.), Geol. Soc. Lond. Spec. Publ. 45, 153–171.

Schmid, S.M., Zingg, A. & Handy, M. 1987: The kinematics of movement along the Insubric Line and the emplacement of the Ivrea Zone. Tectonophysics 135, 47–66.

Schneider, W.A. 1984: Common depth point stack. Proc. Inst. Electric. Electron. Eng. (IEEE) 72, 1238–1254.

Schwendener, H. 1984: Ein gravimetrisches Krusten-Mantel-Modell für ein Profil vom nördlichen Alpenvorland bis an die Ligurische Küste. Geodätisch-Geophysikalische Arbeiten in der Schweiz, Schweizerische Geodätische Kommission 36, 1–160.

Schwendener, H. & Mueller, St. 1990: A three-dimensional model of the crust and upper mantle along the Alpine part of the European Geotraverse (EGT). Tectonophysics 176, 193–214.

Sierro, N.A.M.J. 1988: Regionale Struktur der Erdkruste in der Nordschweiz, PhD Thesis, ETH Zürich.

Spakman, W. 1990: The structure of the lithosphere and mantle beneath the Alps as mapped by delay time tomography. In: Results from the fifth EGT study centre (Roischolzhausen): Integrative Studies (Ed. by Freeman, R., Giese, P. & Mueller, St.), European Science Foundation, Strasbourg, 213–220.

Stäuble, M. 1990: Seismic reflection profiling from the Molasse Basin into the Alps of eastern Switzerland: processing, interpretation and modelling. PhD Thesis, University of Berne.

Taner, M.T., Cook, E.E. & Neidell, N.S. 1970: Limitations of the reflection seismic method – lessons from computer simulation. Geophysics 35, 551–571.

Trümpy, R. 1980: Geology of Switzerland – a Guide Book. Wepf & Co., Basel.

Valasek, P. & Holliger, K. 1990: Approaches towards an integrated interpretation of the NFP20 deep crustal reflection profiles along the Alpine segment of the EGT. In: Sixth EGT Workshop: Data Compilation and Synoptic Interpretation (Ed. by Freeman, R. & Mueller, St.), European Science Foundation, Strasbourg, 137–148.

Valasek, P., Frei, W., Stäuble, M. & Holliger, K. 1990: Processing of the NFP20 seismic reflection traverses across the Swiss Alps by the ETH-Zurich data processing center. In: Deep Structures of the Alps (Ed. by Roure, F., Heitzmann, P. & Polino, R.), Mém. Soc. géol. France 155, Mém. Soc. géol. Suisse 1, Soc. geol. Ital. Vol. spec. 1, 55–64.

Valasek, P., Mueller, St., Frei, W. & Holliger, K. 1991, in press: Results of NFP20 seismic reflection profiling along the Alpine section of the European Geotraverse (EGT). Geophys. J.

Warner, M.R. 1986: Deep seismic reflection profiling the continental crust at sea. In: Reflection Seismology: A Global Perspective (Ed. by Baranzangi, M. & Brown, L.), Amer. Geophys. Union, Geodynamics Series 13, 281–286.

— 1987: Migration – why doesn't it work for deep continental data? Geophys. J.R. astr. Soc. 89, 21–26.

— 1990a: Basalts, water or shear zones in the lower continental crust?, Tectonophysics 173, 163–174.

— 1990b: Absolute reflection coefficients from deep seismic reflections. Tectonophysics 173, 15–23.

Wever, T. 1989: The Conrad discontinuity and the top of the reflective lower crust – do they coincide? Tectonophysics 157, 39–58.

Yan, Q.Z. & Mechie, J. 1989: A fine structural section through the crust and lower lithosphere along the axial region of the Alps. Geophys. J. 98, 465–488.

Zelt, C.A. & Ellis, R.M. 1988: Practical and efficient ray tracing in two-dimensional media for rapid traveltime and amplitude forward modelling. Can. J. Expl. Geophys. 24, 16–31.

Manuscript received 17 January 1991
Revised version accepted 15 April 1991